POLITECNICO DI TORINO
Repository ISTITUZIONALE

Test methods for CO2 mineralization in cement-based materials: A review by RILEM TC 309-MCP

Original
Test methods for CO2 mineralization in cement-based materials: A review by RILEM TC 309-MCP / Matschei, T., Braymand, S., Garg, N., Huet, B., Jansen, D., Myers, R.J., Scruggs, B., Bernard, E., Bertola, J., Cazacliu, B., Ellwood, L., Felten, C., Ferrara, G., Garboczi, E., Gholizadeh Vayghan, A., Hafez, H., Hanein, T., Kanavaris, F., Mahoutian, M., Maruyama, I., et al.. - In: MATERIALS AND STRUCTURES. - ISSN 1359-5997. - 59:4(2026), pp. 1-24. [10.1617/s11527-026-03064-x]

Availability:
This version is available at: 11583/3010671 since: 2026-05-08T09:37:19Z

Publisher:
Springer

Published
DOI:10.1617/s11527-026-03064-x

Terms of use:

This article is made available under terms and conditions as specified in the corresponding bibliographic description in the repository

Publisher copyright

(Article begins on next page)

16 September 2026

Materials and Structures (2026) 59:175
https://doi.org/10.1617/s11527-026-03064-x

RILEM TC REPORT

Test methods for CO_2 mineralization in cement-based materials: A review by RILEM TC 309-MCP

Thomas Matschei · Sandrine Braymand · Nishant Garg · Bruno Huet · Daniel Jansen · Rupert J. Myers · Bruce Scruggs · Ellina Bernard · Julie Bertola · Bogdan Cazacliu · Lucy Ellwood · Christian Felten · Giuseppe Ferrara · Edward Garboczi · Asghar Gholizadeh Vayghan · Hisham Hafez · Theodore Hanein · Fragkoulis Kanavaris · Mehrdad Mahoutian · Ippei Maruyama · Sébastien Roux · Philippe Turcry · Jørgen Skibsted · Ruben Snellings · Sumit Srivastava · Virginie Vial · Jinxin Wei · Maciej Zajac · Zhidong Zhang · Prannoy Suraneni

Received: 25 September 2025 / Revised: 7 March 2026 / Accepted: 16 March 2026
© The Author(s) 2026

Abstract CO_2 can be absorbed and mineralized as solid carbonates in a range of construction materials. Accurate measurement of CO_2 content and uptake in cement-based and other construction products is important for the development as well as the certification of novel mineral carbonation products, processes, and practices. However, measurement is complex as samples can range from fine powders to blocks with varying levels of heterogeneity, different solid carbonate phases can be present, and measurement methods may require correction for interferences. When and where the CO_2 content is measured is also important. Numerous techniques are available for measuring the solid CO_2 content of a sample, from which the CO_2 uptake can be calculated. Here, a critical review of the most relevant methods is presented; the most used methods are thermogravimetric and combustion analysis, however, diffraction-based, spectroscopic, wet-chemical, and other methods can also be used for this purpose. Advantages and disadvantages of the various test methods are discussed. Aspects of sample preparation, result interpretation, measurement limitations and possible interferences, as well as the use of complementary methods are

TC Membership Chair: Ruben Snellings
Deputy Chair: Thomas Matschei

TC Members: Arezou Ahmadi, Abudushalamu Aili, Aleena Alex, Adrian Alujas-Diaz, Stelios Antiohos, Abdullah Anwar, Ignacio Artamendi, Rauno Baese, Elifsu Balci, Aniruddha Baral, Fernanda Belizario Silva, Susan Bernal, Ellina Bernard, Julie Bertola, Andrea Bisciotti, Simon Blotevogel, Sandrine Braymand, Ngoc Kien Bui, Jennifer Canul Polanco, Bogdan Cazacliu, Piyush Chaunsali, Boyu Chen, Seongmin Cho, Özlem Cizer, Nico Coenen, Rachel Cook, Martin Cyr, Vinh Dao, Marco Davolio, Laure Delavernhe, Yuvaraj Dhandapani, Michal Drewniok, Sarra Drissi, Vilma Ducman, Yogarajah Elakneswaran, Lucy Ellwood, Sumesh Erikandath, Christian Felten, Pan Feng, Giuseppe Ferrara, Thomas Feuardent, Edward Garboczi, Nishant Garg, Fabien Georget, Asghar Gholizadeh Vayghan, Anabela Guilarducci, Hisham Hafez, Theodore Hanein, Harald Hilbig, Benoit Hilloulin, Yunlu Hou, Shi Hu, Liming Huang, Bruno Huet, Rachida Idir, Sumin Im, Burkan Isgor, Shafiq Ishak, Daniel Jansen, Roman Jaskulski, Yi Jiang, Fei Jin, Nirrupama Kamala Ilango, Muralidhar Kamath, Fragkoulis Kanavaris, Antonis Kanellopoulos, Mahipal Kasaniya, Xinyuan Ke, Arno Keulen, Mo Kim Hung, Kopitha Kirushnapillai, Hichem Krour, Henning Kruppa, Sanjeev Kumar, Nikhil Kunati, Namkon Lee, Ye Li, Tung Chai Ling, Lin Liu, Diana Londono Zuluaga, Barbara Lothenbach, Monique Lunardi, Zihan Ma, Alisa Machner, Mehrdad Mahoutian, Fabio Maia Neto, Hegoi Manzano, Isabel Martins, Ippei Maruyama, Daniella Mehanni, Tom Moore, Rupert Myers, Sriramya Nair, Hoang Nguyen, Peter Nielsen, Fabian Niewöhner, Leila Nobrega Sousa, Asier Oleaga, Alexander Oliva Rivera, Cédric Patapy, Ravi Patel, Priyadharshini Perumal, Quoc Tri Phung, Natalia Pires Martins, Shawn Platt, Elsa Qoku, Shubham Raj, Pavel Reitermann, Joana Roncero, Sébastien Roux, Gaurav Sant, Bruce Scruggs, Vineet Shah, AG Sharanya, Meenakshi Sharma, Peiliang Shen, Vikash Singh, Priyanshu Sinha, Jorgen Skibsted, Qifeng Song, Lourdes Souza, Sumit Srivastava, Mateja Stefancic, Katarina Ster, Prannoy Suraneni, Arezki Tagnit-Hamou, Marie Joshua Tapas, Tan Tee-How, Karl-Christian Thienel, Sara Tominc, Jean

Published online: 03 April 2026

highlighted. Important aspects of conversion of measured solid CO_2 contents to calculated CO_2 uptake are highlighted.

Michel Torrenti, Philippe Turcry, Neven Ukrainczyk, Ikenna Uwanuakwa, Virginie Vial, Yury Villagran Zaccardi, Anya Vollpracht, Stefanie Von Greve-Dierfeld, Charitha Vootukuri, Mingyu Wang, Wei Wang, Yue Wang, Klaartje De Weerdt, Jinxin Wei, Frank Winnefeld, Hong Wong, Elena Woydich, Zichun Xia, Jin Yang, Noor Yaseen, Guang Ye, Doo-Yeol Yoo, Junjie You, Hao Yu, Maciej Zajac, Nan Zhang, Shizhe Zhang, Zhidong Zhang, Zengfeng Zhao.

Supplementary Information The online version contains supplementary material available at https://doi.org/10.1617/s11527-026-03064-x.

T. Matschei · C. Felten
Institute of Building Materials Research, RWTH Aachen University, 52062 Aachen, Germany

S. Braymand
Laboratoire ICube, Université de Strasbourg, 67081 Strasbourg, France

N. Garg
Civil and Environmental Engineering, University of Illinois Urbana-Champaign, Urbana, IL 61801, USA

B. Huet
Holcim Innovation Center, 95 rue du Montmurier, 38070 Saint-Quentin-Fallavier, France

D. Jansen
GeoZentrum Nordbayern, Friedrich-Alexander-Universität Erlangen-Nürnberg, 91054 Erlangen, Germany

R. J. Myers
Department of Civil and Environmental Engineering, Imperial College London, London SW7 2AZ, UK

B. Scruggs
NIST, Gaithersburg, MD 20899, USA

E. Bernard
Empa, Swiss Federal Laboratories for Materials Science and Technology, Laboratory for Concrete & Asphalt, 8600 Dübendorf, Switzerland

J. Bertola · V. Vial
Vicat, 38080 L'Isle d'Abeau, France

B. Cazacliu
Université Gustave Eiffel, MAST, GPEM, 44344 Bouguenais, France

L. Ellwood · H. Hafez · T. Hanein
School of Civil Engineering, University of Leeds, Leeds LS2 9LG, UK

G. Ferrara
Department of Applied Science and Technology, Politecnico Di Torino, 10129 Turin, Italy

E. Garboczi
NIST Boulder, Boulder, CO 80305, USA

A. Gholizadeh Vayghan
Pirrouet® Research & Technology Group, Vandersanden Steenfabrieken NV, 3650 Dilsen-Stokkem, Belgium

F. Kanavaris
Arup, London W1T 4BJ, UK

M. Mahoutian
CarbiCrete, Montreal, QC H8T 3J5, Canada

I. Maruyama
Department of Architecture, The University of Tokyo, Tokyo 113-8656, Japan

S. Roux
Laboratoire IJL, Université de Lorraine, 54011 Nancy, France

P. Turcry
Laboratoire Des Sciences de L'Ingénieur Pour L'Environnement (LaSIE), La Rochelle Université, 17000 La Rochelle, France

J. Skibsted
Department of Chemistry, Aarhus University, DK-8000C Aarhus, Denmark

R. Snellings
Department of Earth & Environmental Sciences, Department of Materials Engineering, KU Leuven, 3001 Leuven, Belgium

S. Srivastava
CRH, 1083 HL Amsterdam, Netherlands

J. Wei
College of Civil Engineering, Hunan University, Changsha 410082, China

M. Zajac
Heidelberg Materials, 69120 Heidelberg, Germany

Z. Zhang
Institute for Building Materials, ETH Zürich, 8093 Zurich, Switzerland

P. Suraneni (✉)
Civil and Architectural Engineering, University of Miami, Coral Gables, FL 33146, USA
e-mail: suranenip@miami.edu

1 Introduction

There is great interest worldwide in reducing construction-related CO_2 emissions. The construction materials community is increasingly interested in the important area of mineral carbonation to treat or produce building materials with strongly reduced CO_2 footprint. In mineral carbonation processing, CO_2 is bound in solid products and forms stable alkaline carbonates, mostly $CaCO_3$ polymorphs. As the CO_2 is permanently bound and intentionally incorporated into building products, this is considered a form of carbon capture and utilization (CCU), and helps to offset CO_2 emissions within or even beyond the production process. A wide range of mineral carbonation building products are being considered, from finely divided powders to be used as supplementary cementitious materials or fillers for cement and concrete; carbonation cured recycled concrete aggregates; carbonation hardened blocks, bricks or pavers, and more. For each of these products, accurate quantification methods for bound CO_2 content and CO_2 uptake are of utmost importance in both scientific and industrial contexts, for instance to provide a sound scientific foundation for CO_2 reduction accounting as well as for certification, carbon credits and emission trading schemes. A wide variety of analytical methods exist that enable to follow various characteristics of the carbonation process. Thermogravimetric analysis, combustion analysis, Fourier transform infrared spectroscopy, X-ray diffraction (XRD), and wet-chemical analysis methods are all established techniques for studying mineral carbonation processes. Yet, due to inherent limitations associated with a given test method, multiple methods are often combined to obtain reliable results or for verification. For each individual method, factors such as sample pretreatment, sample preparation, and signal interferences or overlapping play an important role, and must be well-understood to obtain accurate results. In addition, there are method-specific instrument settings and set-ups, as well as data treatment and result calculation steps that must be taken into account correctly. To support the further development and introduction of mineral carbonation products, establishment of detailed test procedures for accessible measurement methods is of key importance. As a first step, this paper critically reviews and identifies the most promising measurement methods for CO_2 content and uptake analysis of construction materials and discusses influencing factors, limitations and interferences for each method. We focus largely on calcite, vaterite, aragonite, and amorphous calcium carbonate. Monohydrocalcite, ikaite, magnesium carbonates, iron carbonates, and other related materials are only briefly mentioned as they are relatively uncommon in the carbonation of construction materials. While we are concerned with CO_2 content, we do not focus on CO_2 profile or depth determination. Thus, techniques such as X-ray tomography (both laboratory and synchrotron), neutron imaging, pair distribution function, electron microscopy, and several others are not covered. Finally, this review covers the most commonly used test methods for CO_2 content/uptake determination; less common and emerging methods are not discussed.

2 Thermogravimetric analysis

Thermogravimetric analysis (TGA) is one of the most commonly used methods for CO_2 content measurement. In TGA, a powdered specimen is heated to high temperatures, typically > 900 °C, while the specimen mass is monitored precisely. The powder mass is usually around 10–100 mg, but some equipment suppliers allow to go up to 5 g. The solid is ground down to a specified particle size, typically below 45–63 µm, placed in an inert crucible, and loaded into the instrument. Heating rates are commonly 5–20 °C/min, meaning the test takes 45–180 min, with a further 30–60 min duration for the furnace to cool down. As the temperature increases, various phases decompose, losing H_2O or CO_2, and the mass loss and stoichiometry are used to quantify the amount of the phase present. The mass loss gives the amount of CO_2, while the mass loss converted based on stoichiometry gives amounts of $CaCO_3$ or other carbonate phases. The technique relies on the fact that specific phases have a well-defined, known composition and that specific decomposition reactions occur at well-known temperature ranges. Table 1 presents reaction, dissociation temperature, and mass changes for the most important carbonate phases.

While Table 1 lists ranges, these ranges are broad and are influenced by the temperature ramp rate, the

Table 1 Reaction, dissociation temperature, and mass changes for selected carbonate phases

Material	Reaction	Temperature	Mass change (g/g)	References
Crystalline calcium carbonate (calcite, vaterite and aragonite) $CaCO_3$	$CaCO_3 \rightarrow CaO + CO_2$	650 – 850 °C	0.440	[1, 2]
Amorphous calcium carbonate $CaCO_3.nH_2O$	$CaCO_3.nH_2O \rightarrow CaO + CO_2 + nH_2O$	< 200 °C (H_2O)* 480 –750 °C (CO_2)	~0.150–0.200 ~0.340	[1]
Monohydrocalcite $CaCO_3.H_2O$	$CaCO_3.H_2O \rightarrow CaO + CO_2 + H_2O$	170 – 380 °C (H_2O) 600 – 750 °C (CO_2)	0.180 0.370	[3]
$MgCO_3$	$MgCO_3 \rightarrow MgO + CO_2$	400 – 700 °C	0.522	[4]
$FeCO_3$	$3FeCO_3 \rightarrow Fe_3O_4 + 2CO_2 + CO$	450 – 550 °C	0.334	[5]
$FeCO_3$	$2FeCO_3 + 1/2O_2 \rightarrow Fe_2O_3 + 2CO_2$	450 – 550 °C	0.311	[5]
$NaHCO_3$	$2NaHCO_3 \rightarrow Na_2CO_3 + CO_2 + H_2O$ $Na_2CO_3 \rightarrow Na + CO_2 + ½O_2$	90 –150 °C	0.369	[6]
$KHCO_3$	$2KHCO_3 \rightarrow K_2CO_3 + CO_2 + H_2O$ $K_2CO_3 \rightarrow K + CO_2 + ½O_2$	100 – 160 °C	0.310	[7]

*Additional water may be included which dehydrates at < 200 °C

particle size distribution, the gas composition, amorphous vs. crystalline phases, and the nature of the polymorph present. As an example, the data reported by Radha et al. [1] suggest a significant decrease in the temperature of decomposition of $CaCO_3$ by 80—120 °C when the specific surface area is increased from 1 to 10 m^2/g. The exact choice of temperatures to determine the $CaCO_3$ content and various corrections can become quite complex [8, 9]. Step, tangential and other mass loss integration methods have been proposed, as have corrections for buoyancy [8, 9]. While quantification of amounts of $CaCO_3$ as low as 1% appears to be possible, relative errors are expected to be significant at low contents.

Arguably, in most mineral carbonation products, we are limited to $CaCO_3$, $MgCO_3$ and intermediates thereof, which form under economically accessible conditions. However, the presence of multiple $CaCO_3$ polymorphs and the possible occurrence of amorphous $CaCO_3$ (which decarbonates at lower temperatures between 480 and 750 °C) may complicate the mass loss measurement. Additionally, amorphous calcium carbonates may contain up to 20 wt. % water, which is lost in a temperature range between 50 and 200 °C [1]. The main magnesium carbonate phases occurring in aqueous or moist carbonation are hydrotalcite ($Mg_6Al_2CO_3(OH)_{16}{\cdot}4H_2O$ and similar compositions with a variable Mg/Al ratio) or hydromagnesite ($Mg_5(CO_3)_4(OH)_2{\cdot}4H_2O$). These present CO_2 mass losses below 600 °C, which are intermixed with water and other losses and are difficult to quantify. Using a coupled TGA and mass spectrometry instrument allows to better separate out contributions of amorphous calcium carbonates to mass loss.

TGA suffers from various limitations that are common to all powder-based methods, such as sampling and interference and that are not related to the measurement itself. The main method-related limitation is related to mass loss overlap with other phases, as described above, and precise quantification can be challenging. Various $CaCO_3$ polymorphs cannot be easily differentiated using TGA and other techniques must be used. By its nature, the technique is destructive, and the sample cannot be reused. Use of coarse particles in testing may cause underestimation of carbonates in cases where carbonates are encapsulated by other materials that can be decomposed at higher temperatures [10]. The coexistence of silica gel and carbonate introduces the Hedvall effect, resulting in the decomposition of calcium carbonate at lower temperature ranges, complicating measurement [11].

TGA instruments are widely available in lab-settings, and the TGA is arguably (currently) one of the two most common methods to determine the mineralized CO_2. However, as described above, due to overlaps in decomposition temperatures and the general complexity of cementitious materials, complementary methods are often needed. X-ray

fluorescence spectroscopy enables assessing the precursor chemical composition and can be used to identify the carbonatable components (CaO, MgO, FeO) and helps to estimate the theoretical maximum CO_2 binding potential. Methods such as XRD are also commonly used to complement TGA; through these methods, presence/amounts of phases such as $Ca(OH)_2$, $CaCO_3$, $MgCO_3$ etc., can be determined, which leads to understanding of interferences and further confidence in the measured values of $CaCO_3$ and $MgCO_3$. Additionally, TGA can be coupled with a mass or infrared spectrometer to quantify the amounts of released gasses at a certain temperature range, thus correctly allocating CO_2 related mass loss and allowing to differentiate from other sources of mass loss, e.g. water and sulfate.

Finally, when TGA is unavailable, decarbonation mass losses can be measured using step-wise heating in a lab furnace, like those done in loss of ignition (LOI) test. Ideally, such a test would be done with inert gas flow, and the mass loss over the decarbonation temperature range, e.g., between 550 and 850 °C, can be used to estimate CO_2 or $CaCO_3$ amounts. Such an approach obviously suffers from interferences such as powder instability before or during weighing in a conventional lab balance, and the lack of a mass loss curve makes it less reliable, but it is more practically and widely applicable. This method has the advantage of allowing the use of a much larger sample mass (a few grams) than that of TGA (a few milligrams). The furnace can also be equipped with a balance for continuous monitoring of the sample mass change [12]. It is then similar to TGA but at large scale. Maruyama et al. [13] describe the development of a large-scale thermogravimetric and gas analyzer that can be used to determine CO_2 in concrete. While sample preparation was challenging, the results obtained were in accordance with theoretical values and the experimental duration was relatively short, overcoming some of the challenges described in this section. The throughput and accuracy of TGA for use in larger scale research projects has been reported to be improved by using multi-sample TGA equipment that can test 18 samples at one time with sample weights of 3—4 g [14].

3 Combustion analysis (also known as carbon sulfur (CS) analyzer)

Modern-day combustion analysis is used to quantify carbon and sulfur in a wide variety of materials, including metals, metal alloys, cements, and other materials [15, 16]. The basic principle of combustion analysis is the reaction of oxygen with carbon and sulfur compounds within the sample and quantifying the resultant CO_2 and SO_3 gasses. Early methods of detection of CO_2 involved weighing the CO_2 absorbed on a substrate or various titrimetric methods [17]. Detection of CO_2 by infrared spectroscopy of the combustion gas started in the 1970s and is the predominant method of detection in modern-day automated CS combustion instrumentation. Modern combustion analysis instrumentation is essentially automated "wet chemistry". A simplified schematic of this type of instrumentation is shown in Fig. 1. Other similar equipment can be used for this purpose, as an example, infrared solid carbon analyzers which typically have quartz cells and sucrose calibrations.

The sample is loaded into a ceramic crucible along with various accelerators and fluxing agents needed to drive the combustion reaction to completion. Oxygen gas is used as the carrier/reactant gas. Prior to analysis at the IR detector, the combustion gas is scrubbed of water and SO_3 and any partially combusted CO gas is converted to CO_2 in a secondary oxidation furnace [15]. As sources of carbon contamination are ubiquitous in labs, precautions should be taken to avoid contaminating samples in the preparation process. It is good laboratory practice to fire the ceramic crucibles at a minimum of 1000 °C in air prior to use and then store in a laboratory desiccator.

Specimens are tested in powder form, generally powdered below 150 μm, and weighing around 0.2 g. Prior to analysis, the specimen should be dried to provide a reproducible mass basis to calculate the CO_2 mass fraction. For accuracy of measurements, calibration must be performed using known, standard, high-purity materials with a wide range of CO_2 amounts.

There are very few, if any, reference materials available with the CO_2 mass fraction to cover the range of CO_2 measurements expected in cement-based and other construction materials. National Institute of Standards and Technology (NIST) is engaged in an effort to produce research grade reference materials to support upcoming interlaboratory

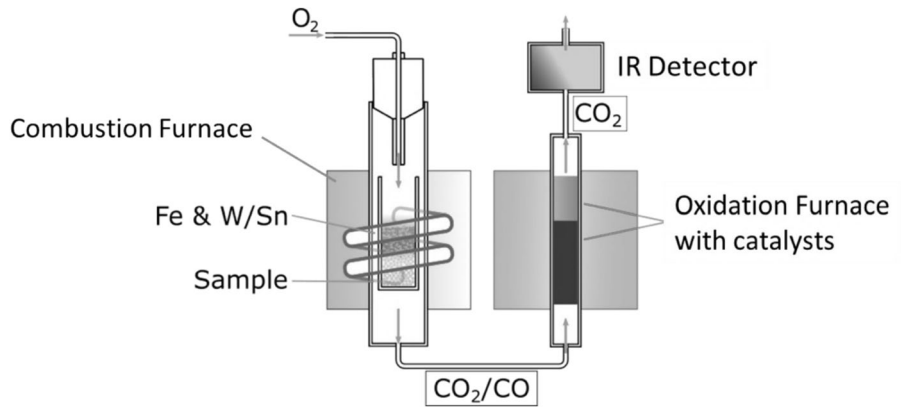

Fig. 1 Simplified schematic of a combustion analyzer showing carbon combustion products (adapted from [18])

studies for an ASTM test method for using combustion analysis for cements and concretes [19]. A validation method for CO_2 measurement is described in ASTM C114 [15], however, it seems suited to lower mass fractions of CO_2.

Over the course of several days, repeatability measurements in a single lab, single operator study yielded about 2% relative repeatability on standard reference materials [19]. The measured values of mass of carbon have to be converted to mass of CO_2, based on stoichiometry; further corrections are needed based on existing carbon if uptake should be determined. We note that such conversions and corrections are also needed for TGA and other methods.

Combustion instrumentation is widely available in many laboratories thanks to their moderate cost, the ease of sample preparation and the speed of analysis. It is arguably, together with TGA, the most commonly used method to determine mineralized CO_2 content. Modern instrumentation can analyze a single sample in about 2 min or less, conferring the method with a distinct speed advantage over TGA.

As the main limitation, combustion analysis has no direct capability to determine carbon speciation. All of the carbon in a completely combusted sample will be converted into CO_2 gas regardless of its initial form. As such, if it is desired to measure the CO_2 uptake of a mineral carbonation product, it is necessary to make measurements before and after the carbonation steps. It should be noted that the stoppage of hydration and preparation of the sample by using isopropanol or other organic material may cause quantification error for combustion and other methods [10, 20]. Differentiation of mineralized and other forms of carbon, including organic carbon from admixtures, additives or incomplete pre-combustion e.g. in fly ashes, is not possible in combustion-based methods as-is. However, it is possible to add additional sample preparation steps to differentiate the carbonate content from organics by acidifying the sample to drive off CO_2 mineralized in the form of carbonates [21]. Differentiation of $CaCO_3$ and $MgCO_3$ or other metal carbonates is not possible in combustion methods. Similar to TGA, the method is destructive.

4 Solid-state nuclear magnetic resonance spectroscopy

Solid-state nuclear magnetic resonance (NMR) spectroscopy, employing magic-angle spinning (MAS), has been widely used in studies of cement-based materials [22–25], where it has been utilized as the method probes one nuclear spin isotope at a time and because amorphous and crystalline phases are both detected in an equal manner. ^{27}Al and ^{29}Si NMR can be used to assess various changes in the cement paste over the carbonation process (Fig. 2), such as decalcification of the C-(A)-S–H phase, structural studies of the formed alumina-silica gel including aluminum coordination, and investigations that probe the pozzolanic reactivity of the alumina-silica gel in new cement formulations [26, 27].

^{13}C MAS NMR allows detection of the calcium carbonate polymorphs, calcite, aragonite, and vaterite, which give ^{13}C resonances at 168.8, 171.2, and 168.7 ppm, respectively [28, 29], as illustrated in Fig. 2 by the detection of calcite in a carbonated cement paste. Moreover, $^{13}C\{^{1}H\}$ cross-polarization (CP) NMR experiments, where magnetization is transferred from ^{1}H to ^{13}C, allow detection of hydrous carbonate species, e.g. on the surface of

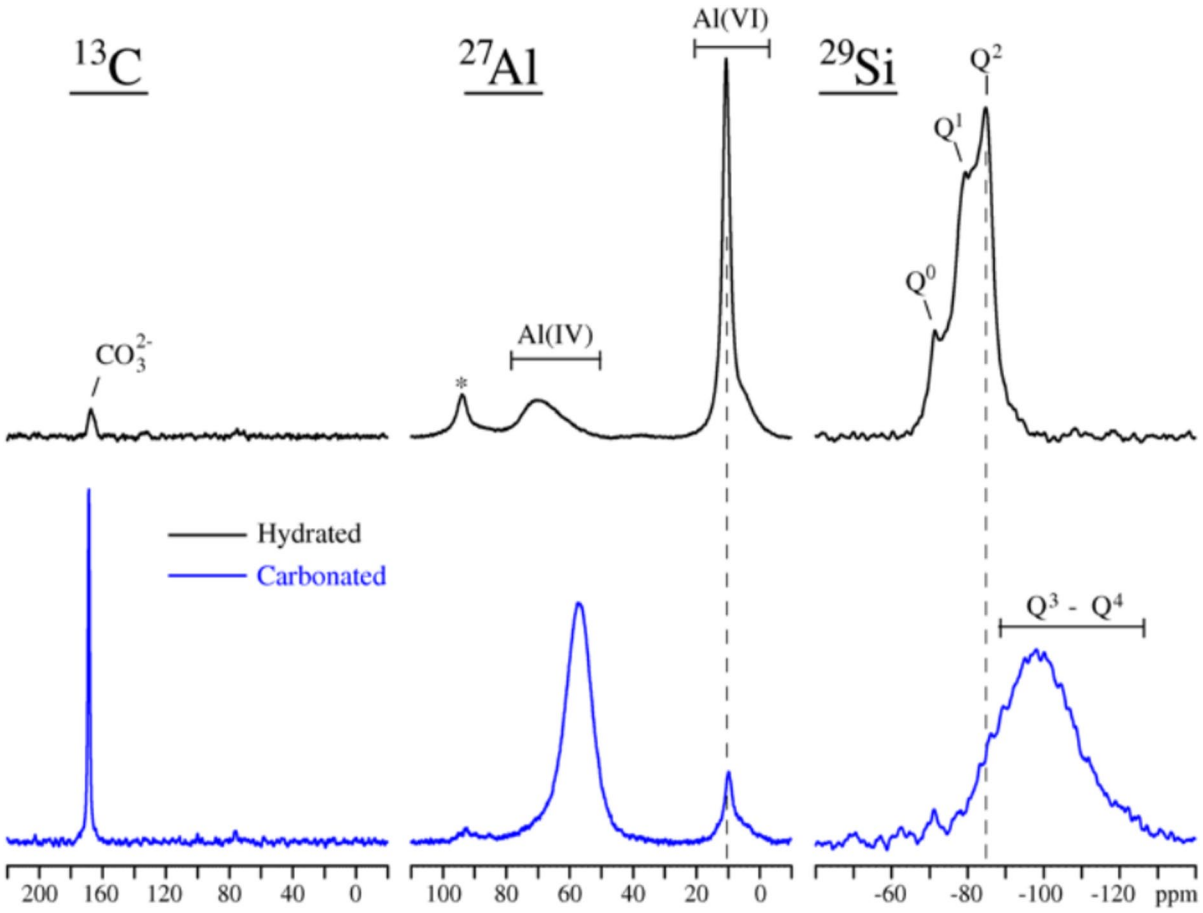

Fig. 2 ^{13}C, ^{27}Al, and ^{29}Si MAS NMR spectra of a well hydrated Portland cement paste before and after aqueous carbonation for 360 min (reproduced from [26], CC BY 4.0)

$CaCO_3$ particles, and of amorphous calcium carbonate ($CaCO_3 \cdot nH_2O$) [30] despite its resonance is overlapping with the peaks from the crystalline $CaCO_3$ polymorphs.

Solid-state NMR analyses are generally performed on dry, powdered samples and require sample amounts of 25—250 mg, depending on the nucleus under investigation and the special setup in terms of attainable MAS spinning frequencies (*i.e.* NMR probes and rotor diameters) [25]. The method is non-destructive but also associated with low sensitivity. Thus, the low natural abundance of ^{13}C (1.1%) and ^{29}Si (4.7%), combined with their generally long relaxation times (T_1) implies that ^{13}C and ^{29}Si NMR experiments typically require overnight acquisitions to achieve acceptable signal-to-noise ratios. Another limitation of the method is the sensitivity to high levels of paramagnetic ions (*e.g.* Fe), which will result in an efficient relaxation of magnetization that may prevent detection of the signals. This may be a challenge for carbonated materials containing large quantities of fly ash or steel slag with high levels of iron. An absolute quantification of CO_2 uptake in the form of $CaCO_3$ can be accomplished by solid-state ^{13}C MAS NMR, however, the experiments would be rather time consuming, considering the generally long T_1 relaxation time for ^{13}C in carbonate ions along with the low natural abundance of the isotope, among other reasons.

Magnesium carbonates have been studied using ^{13}C MAS NMR and a detailed understanding of magnesium carbonate phases and M-S–H in complex systems can be obtained by combining Fourier-transform infrared spectroscopy, XRD, and NMR

[31]. Solid-state ^{13}C NMR has been shown to be able to distinguish various magnesium carbonate phases, such as magnesite, hydromagnesite, dypingite, and nesquehonite [32].

5 Fourier-transform infrared spectroscopy

Fourier-transform infrared spectroscopy (FTIR), which provides information about the different molecular species present in any sample, is a common infrared spectroscopy method. FTIR has been used to quantify depth of carbonation for concrete durability studies [33]. Combining XRD and FTIR, authors claimed to identify amorphous calcium carbonate in hydrated ternary cements and aragonite in the systems post-carbonation [34]. In studies evaluating the effects of carbonation and carbonation curing, authors identified using FTIR, microstructural modifications, including calcium hydroxide carbonation, C–S–H decalcification, and the formation of calcite, vaterite, aragonite, and amorphous calcium carbonates [35]. The progress of the enforced carbonation process, i.e. the increase in the calcium carbonate content, for various material streams could be followed in a qualitative manner using FTIR [36, 37]. FTIR can also be potentially used to quantify $CaCO_3$ amounts [38].

$CaCO_3$, depending on the polymorph and phase, shows various IR absorption bands between 600 and 1500 cm^{-1}, as summarized in Table 2 [39–47] for the following vibrations: symmetric stretching ($\nu 1$), out-of-plane bending ($\nu \mathbf{2}$), asymmetric stretching ($\nu \mathbf{3}$), and in-plane bending ($\nu 4$). Figure 3 shows FTIR spectra for calcite, aragonite, and vaterite [40]. In simple (model) systems, the absence of $\nu 1$ can be used to differentiate calcite from aragonite/vaterite, the shift in $\nu \mathbf{4}$ to identify vaterite, etc., however, this is complex in cementitious systems due to overlap from aluminosilicate and other bonds. Thus, in most studies, it is common to combine FTIR with complementary techniques, including XRD, TGA, and Raman, among others. FTIR absorption bands of $CaCO_3$ polymorphs can vary slightly depending on measurement conditions, instrument calibration, and sample characteristics, further highlighting the importance of using multiple techniques.

The most common FTIR types are transmission FTIR and ATR-FTIR (attenuated total reflectance mode). For the first method, sample preparation for solids requires KBr pellets. ATR-FTIR is an attractive measurement, which is rapid (measurement only takes 1–2 min) and does not require any sample preparation beyond a clamping arm that applies pressure on the powder. Powder is extracted from the paste, mortar, concrete, ground to cement or similar fineness, and tested using FTIR. Less than 0.5 g of powder is adequate for FTIR testing. Issues with sampling and aggregate interference are similar as with TGA and other powder methods, and discussed later. FTIR spectra of raw materials can help understand and minimize interferences from pre-existing $CaCO_3$.

The main limitation of FTIR is that, it is for the most part, only qualitative. Through careful processing, calibration, and accounting for matrix effects, quantification in cementitious materials was demonstrated in a recent study [38], and further studies could advance FTIR quantification. Poor signal-to-noise, weak peaks, and peak overlap are other major limitations. These could be overcome through careful sampling, selective dissolution, subtractive comparisons, and combining data with other complementary techniques. The test can be destructive or non-destructive, depending on exactly how it is performed.

The ($\boldsymbol{\nu}_2, \boldsymbol{\nu}_3, \boldsymbol{\nu}_4$) modes of calcite, dolomite, and magnesite can be differentiated [48], and therefore,

Table 2 Band positions (cm^{-1}) and assignments of common $CaCO_3$ phases in cementitious systems [39–47]. Peaks which are typically weak are identified with a 'w'

Phase	Composition	$\nu 1$	$\nu 2$	$\nu 3$	$\nu 4$
Calcite	$CaCO_3$	-	874	1420	713 w
Aragonite	$CaCO_3$	1083	844/854	1461	700/712
Vaterite	$CaCO_3$	1087 w	876	1476	744 w
Amorphous calcium carbonate	$CaCO_3.xH_2O$	1067	864	1492	690/725 w
Monohydrocalcite	$CaCO_3.H_2O$	1063 w	872	1492	698
Ikaite	$CaCO_3.6H_2O$	1085 w	876	1425 w	720 w

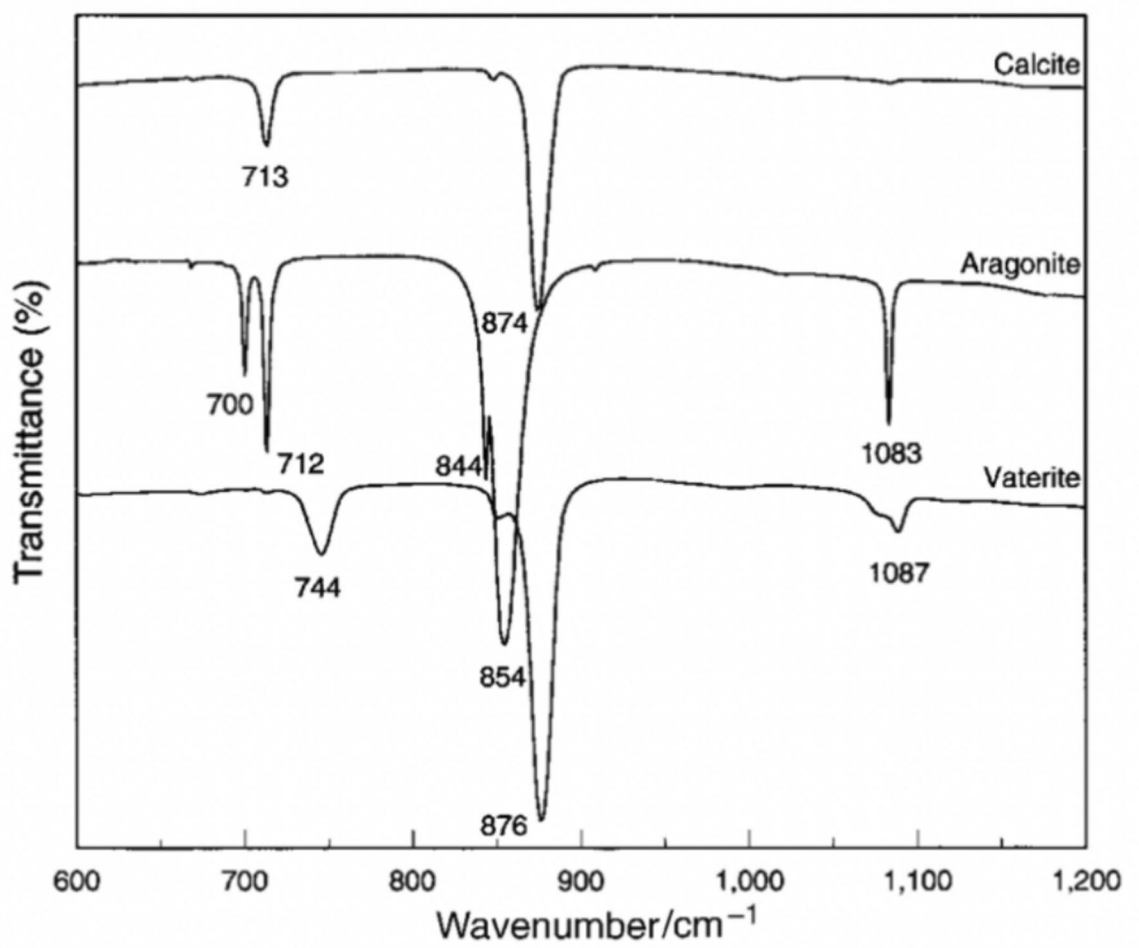

Fig. 3 FTIR spectra for calcite, aragonite, and vaterite (reproduced from [40])

these minerals can be differentiated in FTIR, at least in simple systems. FTIR has also been used to distinguish different members of the siderite-magnesite solid-solution series using shifts in the 1430 cm^{-1} and 880 cm^{-1} bands [49].

6 Raman spectroscopy & imaging

Raman spectroscopy and imaging have emerged as valuable tools for assessing the carbon uptake in cementitious systems. They have been widely used to measure the carbonation level at different depths [50], obtain the composition of carbonated cement paste [51], and investigate the biomineralization processes involving amorphous calcium carbonate [52]. Various polymorphs of calcium carbonate formed during carbonation can be identified using Raman spectroscopy [53, 54]. Table 3 summarizes band positions for common carbonate phases. As with FTIR, some variability in the exact positions can occur.

Calcium carbonates have a strong Raman scattering between 1080 and 1090 cm^{-1} (ν_1 peak), corresponding to the symmetric stretching of C-O bonds [55]. Additional (ν_2, ν_3, ν_4) modes provide further insights into different calcium carbonate species including amorphous phases [52, 56]. Figure 4 illustrates the unique Raman spectra of some of the common calcium carbonate phases. Hence, Raman spectroscopy's high sensitivity to crystalline and amorphous phases enables accurate phase

Table 3 Band positions (cm^{-1}) and assignments of the carbonate phases identified in cementitious systems [52, 55–58]

Phase	Composition	ν_1	ν_2	ν_3	ν_4	LV
Calcite	$CaCO_3$	1085 vs	–	1450 vw	712 w	280 m
Aragonite	$CaCO_3$	1085 vs	853 vw	–	700 vw	205 w
Vaterite	$CaCO_3$	1074 m	–	–	740 vw	300 w
Amorphous calcium carbonate	$CaCO_3.xH_2O$	1077 s	868 vw	1390 vw	698 w	–
Monohydr-ocalcite	$CaCO_3.H_2O$	1069 m	–	–	–	–
Ikaite	$CaCO_3.6H_2O$	1072 vs	873 w	–	–	–

vs: very strong, s: strong, m: medium, w: weak, vw: very weak

identification at high resolution [50]. Moreover, Raman imaging provides valuable spatiotemporal information on the carbonation of structural components in concrete (Fig. 4).

Capturing images at different locations and time points, Raman imaging allows an understanding of the distribution, depth, and extent of carbonation in concrete structures. While Raman imaging itself is generally non-destructive, the core of the concrete is required to assess the carbonation profile across the cross-section of the concrete [50].

Several studies have successfully employed Raman spectroscopy and imaging to monitor and quantify carbonation in cementitious systems [50, 52, 59, 60]. For instance, a portable Raman spectrometer has been used to study the kinetics of carbonation of portlandite, enabling the detection of the carbonation front through principal component analysis [60]. Raman spectroscopy has been employed for monitoring the evolution of several phases during natural carbonation [53]. Additionally, the correlation between carbonate content and Raman peak intensity has demonstrated a good agreement with conventional techniques [50]. Furthermore, Raman imaging has been employed to monitor the spatial and temporal evolution of calcite and portlandite in cement pastes over 14 days on a large area (1 mm × 1 mm) [59].

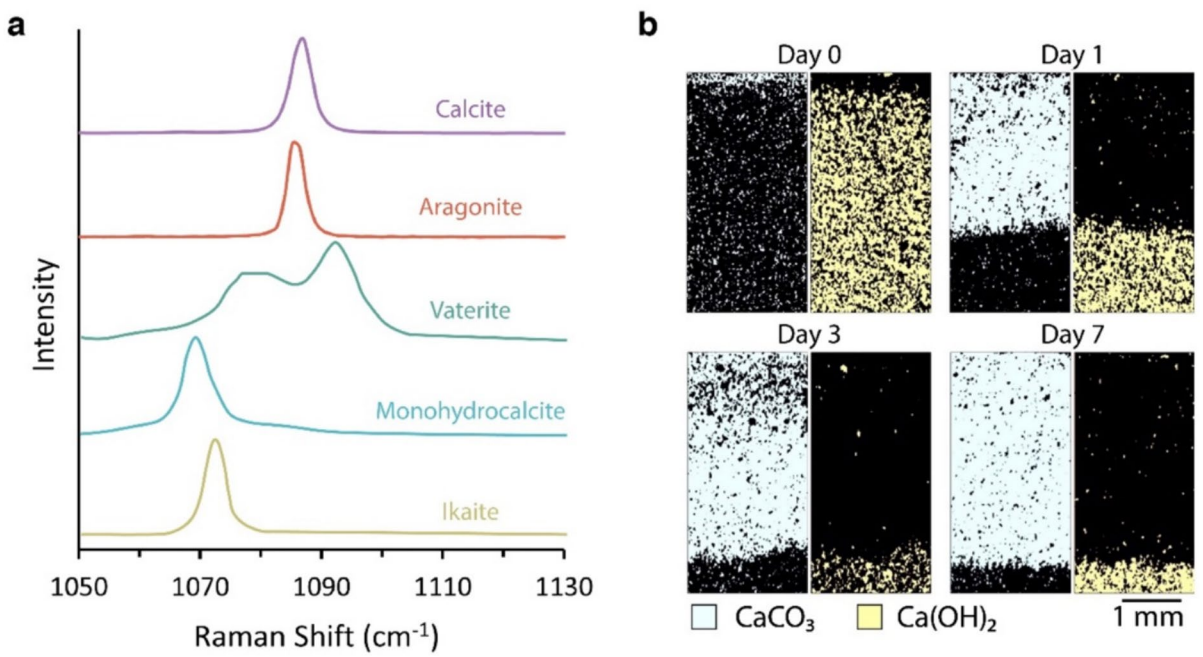

Fig. 4 **a** Raman spectra of different $CaCO_3$ phases, calcite aragonite, vaterite, monohydrocalcite, and ikaite (adapted from [54]); **b** Raman phase maps (1.8 × 3.6 mm) of calcite and portlandite on a hydrated cement paste specimen (w/c of 0.4) subjected to carbonation (adapted from [59])

To obtain high-quality data, it is preferred to use polished samples with low roughness [61]. Complications in data analysis can arise due to poor signal-to-noise ratio and overlapping peaks. However, these challenges can be mitigated by optimizing the scan parameters and performing thorough spectral analysis. Challenges that warrant further investigation include the long duration of scan time for accurate quantification via large-area scans [62], other scanning parameters, and the selection of an adequate representative area for analysis. Moreover, further investigation on the quantification methods for the carbon uptake capacity of various cementitious systems over a representative area is required.

Magnesite, similar to calcite, shows (ν_1, ν_3, ν_4) bands, and ν_4 of magnesite, at 738 cm^{-1} is significantly different from that of the 712 cm^{-1} band of calcite to enable differentiation [63]. Raman spectroscopy has also been shown to be able to differentiate various members of the siderite–magnesite anhydrous solid solution series [64]. Hydromagnesite and other phases have been studied using Raman spectroscopy [65], however, disorder, ionic substitution, and co-existence of phases make analysis and obtaining high quality spectra using solely Raman challenging. Combining Raman analysis with complementary techniques such as XRD is recommended for unambiguous identification and quantification. Recently, Rathnakumar and Garg [66] conducted multi-modal imaging on the carbonation front where multiple techniques like laser profilometry, contact angle goniometry, XRD, and TGA were combined with Raman Imaging to record evidence of pore refinement upon carbonation [66].

7 X-ray diffraction

X-ray diffraction (XRD) is an analytical technique widely used to identify and quantify crystalline phases in powders. In quantitative phase analysis, the presence of amorphous phases is taken into account by comparison to internal or external standards or by external calibration. Similar to other powder methods, the measurement of CO_2 uptake by XRD is indirect and based on the quantification of individual crystalline carbonate containing phases. An important limitation and bias of XRD analysis is that CO_2 in amorphous phases is not detected. Typically, XRD is able to detect and quantify crystalline phases present in levels above 0.5–1 wt.% in multiphase mixtures. Multi-laboratory precision of XRD is at the 1 wt.%-level in favorable cases, but may increase in complex mixtures such as Portland cement to up to 5 wt.% for major phases. No dedicated studies on determination of precision or bias of CO_2 uptake measurements by quantitative XRD have been reported.

The measurement principle of XRD is based on the elastic interaction of X-rays with the electron density of atoms situated in a crystal lattice. The diffraction pattern is mainly determined by the symmetry and dimensions of the crystal lattice, the type and the positions of atoms in the unit cell. Using the characteristic combination of peak positions and intensities, crystalline phases can be identified. The well-known Rietveld method uses and refines crystal structure information to fit a calculated pattern to a measured powder diffraction scan. In addition, it is widely used to measure phase abundancies in multi-phase materials, such as cements or carbonated materials.

Figure 5 shows an example of aqueous carbonated C_2S where XRD enabled to detect calcite and vaterite as the main carbonate phases. This clearly highlights the complementarity of XRD to other techniques that cannot distinguish among different $CaCO_3$ polymorphs.

The identification and quantification of carbonate phases formed strongly depends on the raw material. In single phase systems, the identification and quantification of carbonate phases is straightforward without problems caused by peak overlapping. However, for many real materials, such as carbonated cement or steel slag, peak overlap may be severe and require analysis using full-pattern fitting. Figure S1 shows the XRD patterns of carbonated C_2S and carbonated steel slag. The identification of calcite and vaterite in the C_2S system is quite clear, while the identification of the calcite and Mg-calcite peaks in the steel slag system is much more challenging due to the multiphase nature of the raw material containing phases including bredigite, cuspidine, donathite, and more.

Powder XRD is a destructive method. It is mandatory that the particle size distribution of samples is very fine, preferably below 10 µm, to avoid bias and overestimation of amorphous content [68]. Consequently, the sample has to be milled while taking care that the material is not altered by the milling action. For a typical measurement in reflection mode, around

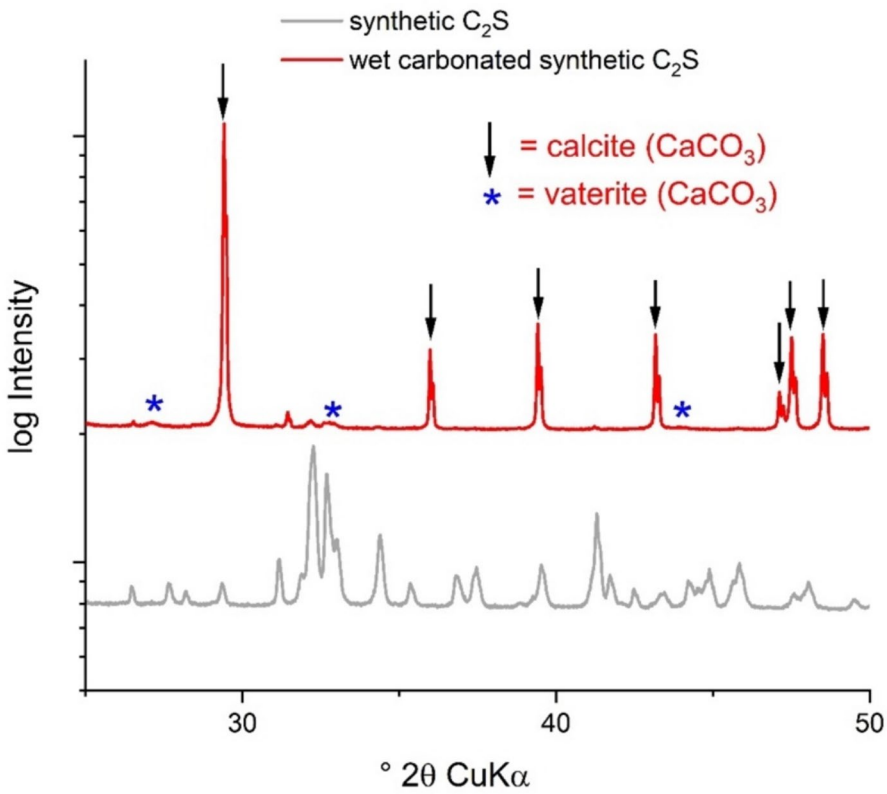

Fig. 5 Synthetic C_2S aqueous-carbonated in 100% CO_2 atmosphere at atmospheric pressure and with excess of water (using data from [67])

2 g of sample are needed. As with other powder methods, care should be taken that the sample measured is representative of the material to be tested.

Identification of crystalline phases or qualitative interpretation of powder XRD data is straightforward using commercial or free software in combination with suitable identification databases. Built-in search/match routines can be combined with a custom-made list of carbonate phases that are likely present. In principle, XRD can be used to detect carbonation reactions in a range of binder systems, since both crystalline reactants (e.g., portlandite, C_2S, tobermorite) and crystalline products (e.g., calcite, aragonite, vaterite) can be identified and measured. Qualitative XRD analysis showed that an investigation of carbonation depth using phenolphthalein in concrete yielded depth values about half as large as carbonation reaction products detectable by XRD [33]; however, other studies showed similar depths [69, 70]. Qualitative XRD was also used to study qualitatively the enforced carbonation of cement fines by tracing the formation of crystalline calcite during carbonation [59, 71, 72].

Quantitative analysis of XRD data is more challenging and commonly done using the Rietveld method implemented in a range of software packages. As a result, individual phase abundancies are obtained. As amorphous phases can be present initially or formed during the carbonation processes, quantitative XRD analysis should not ignore these for the phase contents to be reliable. To quantify the amounts of amorphous phases, either internal standards [37, 68] or external standards approaches [73, 74] are commonly used. If the external standard method is chosen, the chemical composition of the samples, including the H_2O and CO_2 contents, are needed [74]. This may preempt the need for a measurement of CO_2 uptake by XRD. However, since the difference in X-ray absorption between CO_2 and H_2O is not significant, a simple measurement of loss on ignition can be used as well to calculate the sample mass attenuation. This information and calculation are not needed in the internal standard approach, that, in turn, requires careful mixing and homogenization of the chosen internal standard into the material. When operating in transmission geometry, where a

well-defined sample volume is irradiated, an internal standard should be used, because achieving exactly the same packing density for the external standard and the sample is practically not feasible.

In Bragg–Brentano diffractometry, however, an external standard can be applied. In this geometry, the effective irradiated sample volume varies with the diffraction angle, and—due to the comparatively high mass attenuation coefficients of cementitious materials—the specimen is not fully penetrated down to the sample holder. Since air is essentially "invisible" to X-rays compared to the solid phases, differences in packing density between the external standard and the specimen do not play a decisive role in this case.

Several studies have been published using quantitative XRD to quantify enforced carbonation of materials. In [75], hydrated cement paste was exposed to enforced carbonation for up to 30 h and the evolution of different mineral phases was determined by Rietveld analysis (Figure S2). For determination of the amorphous content, the external standard method (rutile) was used. Salman et al. [76] used the internal standard method (with ZnO) to determine the phase composition including the amorphous phase content of a steel slag carbonated under different conditions. Other studies have also used corundum (Al_2O_3) as the internal standard method for amorphous phase determination [77, 78]. As stated in [79], ZnO can be preferred over corundum due to stronger reflections and the absence of X-ray amorphous material.

If calcite is formed during carbonation of Mg/Fe containing systems, a Mg/Fe containing calcite can be formed. Solid solutions of Mg/Fe can be identified by lattice parameter shifts of the calcite formed [80]. During Rietveld refinement several other issues must be considered such as preferred orientation, over-grinding and peak broadening during milling of the samples [81]. Table S1 presents a list of carbonate phases commonly formed during carbonation processing as well as recommendations concerning the ICSD structures to be used for Rietveld refinement.

8 Chemical methods

Chemical methods for quantifying CO_2 are based on reactions between the material and a reagent, allowing for estimates of the CO_2 content. In case of aqueous carbonation, it may be necessary to determine the initial CO_2 value by calculation [82].

The most commonly used chemical method is based on reacting the carbonates with acid and assessing the amount of CO_2 released; this is known as calcimetry (or gasometric analysis). For a mineral containing metal carbonates, the reaction with HCl is governed by the following rapid reaction Eq. 1 (where M equals Ca, Mg, or Fe).

$$MCO_3(s) + 2HCl(aq) \rightarrow MCl_2(aq) + H_2O(l) + CO_2(g) \quad (1)$$

The acid digestion reaction is applicable for Portland cement, blended cements, magnesium-based cements, and other materials. In some cases, a secondary and slower reaction occurs. An example for the acid digestion for dolomite is shown in Eq. 2:

$$CaMg(CO_3)_2(s) + 4HCl(aq) \rightarrow CaCl_2(aq) + MgCl_2(aq) + 2H_2O(l) + 2CO_2(g) \quad (2)$$

In calcimetry, the volume of CO_2 released can be quantified, when the test is carried out at constant atmospheric pressure using the Bernard or Dietrich-Frühling calcimeters. Alternatively, the pressure variation can be measured when the test is carried out at constant volume using a carbonate bomb setup (or carbometer). Such tests are commonly used by geologists to determine the purity of limestone [83, 84]. Tests need to be performed on milled samples of around 1 to 2 g, and are destructive. The calcimeter test, illustrated in Fig. 6a, is specified by the French standard NF P 94–048 [85] and the British Manual of Soil Laboratory Testing [86]. The "carbonate bomb" apparatus (Fig. 6b) is based on the work of Müller [87]. The carbonate bomb requires an initial measurement of a $CaCO_3$ reference standard.

Chemical methods can be based as well on a gravimetric principle where the amount of CO_2 is measured by total weight loss after reaction with acid, assuming the conservation of produced water [89]. In that case, tests can be performed on milled or crushed samples of around 10–30 g. It is a destructive method as the sample must be extracted from the carbonated material [90, 91]. The test is performed by stirring the solution in a conical flask covered with a watch glass and weighing at regular intervals. To allow the volatilized CO_2 to escape from the flask, the glass bell is removed for a few seconds before each weighing. The

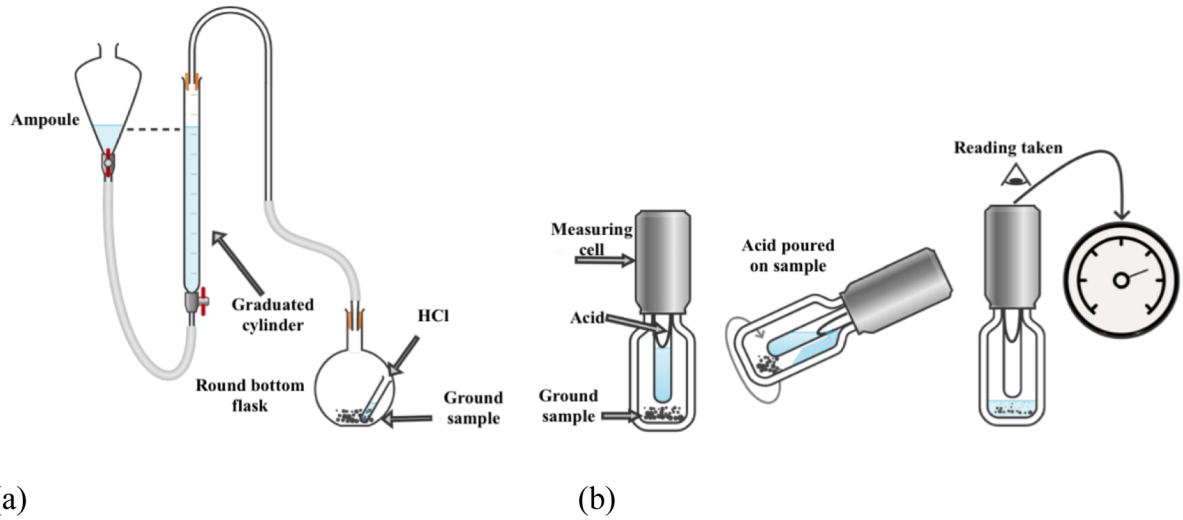

Fig. 6 **a** Bernard calcimeter, adapted from ([85, 86, 88]; **b** carbonate bomb (adapted from [87])

test is carried out until the weight loss between two consecutive values is negligible [92]. As silica gel may hinder the dissolution of encapsulated carbonates, finer samples may have to be used [10]. The test has been used recently to assess CO_2 sequestration in aqueous carbonation of electric arc furnace slag and cement by-pass dust [93, 94].

The digestion-titration method uses a two-step acid-digestion and titration method with a simplified digestion apparatus wherein, at reduced pressure, an acid is added to liberate the chemically bound CO_2 in the specimen (Eq. 1) which is then consequently dissolved in a pre-prepared $Ba(OH)_2$ solution. Following digestion, titration and back-estimation of the specimen CO_2 content are performed using an end-point indicator (e.g., phenolphthalein) and the chemical reaction stoichiometry of the overall process. This method was first developed in the early 1900s by Van Slyke for clinical biochemical studies, but is applicable to carbonates in general [95]. Thien et al. [96] made a slight modification to the specimen holder to avoid errors associated with excessive bubbling during digestion. The apparatus is shown in Figure S3.

Acid digestion can also be used in association with other methods for CO_2 determination. For example, the acid reaction can be coupled to a non-dispersive infrared analyzer to quantify total inorganic carbon (TIC). Tests are performed on 50–100 mg of carbonated samples (< 160 µm) digested with orthophosphoric acid [97] or other acids and then heated to 200 ^{o}C for determination of TIC in the evolved gas flow.

The acid concentration in the tests is chosen so as to guarantee an excess of acid during reaction with MCO_3 but also with the other components of the mineral. Temperature and pressure corrections, or calibration with a calcite standard, are required for calcimeters [98]. The accuracy of the volume reading of the calcimeter is ±0.25 ml CO_2 released, equivalent to 1 mg $CaCO_3$. The accuracy of the pressure reading of the calcimeter expressed as carbonate content is ± K*0.5% $CaCO_3$, where K is the calibration coefficient [99]. For gravimetric estimates, the weight of the released CO_2 is estimated with an accuracy of ± 0.01 g. For the digestion-titration method, the accuracy of the method is directly related to the titrant drop size during titration. Baseline titrations help improve the accuracy of results [96].

As part of the FastCarb project [98–101], recycled concrete aggregates were carbonated on an industrial scale and the CO_2 uptake was determined by calcimetric methods which were found to be accurate for estimating the process efficiency of the carbonation process. They offered average repeatability, a good reproducibility for the calcimeter, and even better for the carbonate bomb. The calcimeter was more accurate when samples were tested in the laboratory as opposed to the carbonate bomb which is more suitable for on-site testing [98, 99].

In many cases, it is assumed that the temperature is kept almost constant while testing. If this is not the case, cooling is required to compensate for the highly exothermic reaction [98, 99]. In the case of high CO_2 levels, sampling is reduced to ensure an excess of acid, which may result in an insufficiently representative unit volume of the sample if its composition is heterogeneous. The presence of sulfides can produce a parasitic reaction, and filtering and other solutions are required to overcome this issue. A major concern for the carbonate bomb is that it is not adapted for samples with a carbonate content of less than 25% because the calibration coefficient of the carbonate bomb is less reliable for this measurement range. Detailed studies of other calcium carbonates, magnesium, and iron carbonates using calcimeteric methods appear unavailable.

9 Carbon uptake and calculations

Reliably quantifying the climate change mitigation potential of mineral carbonation technologies requires accurate measurement of the CO_2 uptake of mineral carbonation products and the correct use of the results in rigorous life cycle assessment (LCA) studies.

The theoretical CO_2 uptake (or binding capacity) of a material is determined by the availability of alkali earth and alkali elements for carbonation. It is commonly calculated using the Steinour equation based on oxide mass % and molar mass, shown in Eq. 3 [102].

$$Theoretical CO_2 uptake(wt\%) = \frac{M_{CO_2}}{M_{CaO}}\left(CaO - \frac{M_{CaO}}{M_{CaCO_3}}CaCO_3\right) + \frac{M_{CO_2}}{M_{MgO}}\left(MgO - \frac{M_{MgO}}{M_{MgCO_3}}MgCO_3\right) + \frac{M_{CO_2}}{M_{Na_2O}}Na_2O + \frac{M_{CO_2}}{M_{K_2O}}K_2O \quad (3)$$

Equation 3 accounts for the wt.% of CaO, MgO, Na_2O, and K_2O available for carbonation and includes the oxide/carbonate molar masses to compute the theoretical (maximum) CO_2 uptake. However, the actual amount of CO_2 uptake varies depending on the waste and carbonation sources used. Much data [26, 103, 104] shows that calcium sulfate will not carbonate at ambient temperature. Na_2CO_3 and K_2CO_3 are soluble, meaning CO_2 is not stored in these phases. While hydrated magnesium carbonate can form by carbonating MgO, this phase is not observed after carbonating PC paste; rather, MgO is stabilized in hydrotalcite [104]. Taking these factors into account, Eq. 3 can be rewritten as Eq. 4.

$$Theoretical CO_2 uptake(wt\%) = \frac{M_{CO_2}}{M_{CaO}}\left(CaO - \frac{M_{CaO}}{M_{CaCO_3}}CaCO_3 - \frac{M_{CaO}}{M_{SO_3}}SO_3\right) \quad (4)$$

When pressurized CO_2 is used, carbonation of $CaSO_4$ [105] and MgO can occur, even though MgO carbonation is usually limited [106]. In this case, the equations above can be modified through the reconsideration of the SO_3 and MgO terms.

When powders are being carbonated, the degree of carbonation can be defined as the difference between the sample weights before and after carbonation with respect to the initial mass of the adopted dry powder. This method is suitable for carbonation of compact samples in CO_2 chambers. However, water release associated with the carbonation reaction should be taken into account and corrected for; a conservative estimate using masses before and after carbonation and the lost mass is shown in Eq. 5 [107, 108].

$$CO_2 uptake(\%) = \frac{Mass_{aftercarb.} + H_2O_{lost} - Mass_{beforecarb.}}{Mass_{beforecarb.}} \quad (5)$$

In many cases, the CO_2 assessment is directly executed on a sample extracted from the mineralized product rather than during the CO_2 absorption process, so the initial mass of the sample before the carbonation is unknown and some assumptions are required to define the CO_2 uptake. In this case, the CO_2 uptake can be related to the total mass of the carbonated sample [97]. For assessing CO_2 uptake using thermal treatment such as TGA, the initial mass before carbonation can be assumed as the mass of the carbonated sample after treatment at specific temperature values, such as 105 °C [109, 110], 800 °C [111], or 950 °C [112]. The use of temperature values higher than the decomposition temperature of

calcium carbonate (~750 °C) is more appropriate as it provides an estimate of the initial mass after the release of the CO_2 content. In many studies the initial mass before the carbonation is defined as the difference between the carbonated mass and its CO_2 content, as shown in Eq. 6 [97, 106], considering the CO_2 contents of the carbonated (final) and raw (initial) materials. This approach exclusively considers weight changes induced by CO_2 uptake. It is important to note that the measurement of CO_2 uptake can be subject to under- or overestimation if concomitant reactions during carbonation, including dehydroxylation or hydration, induce significant mass changes [109].

$$CO_2 uptake(wt\%) = \frac{CO_{2,final}(wt\%) - CO_{2,initial}(wt\%)}{100 - CO_{2,final}(wt\%)} \quad (6)$$

A key parameter to quantify the carbonation is the carbonation efficiency (or the carbonation degree), which is defined as the ratio between the captured mass of CO_2 and the theoretical CO_2 sequestration potential assessed using the Steinour equation [113].

Measurement of CO_2 uptake can be executed at the industrial scale, although few methods have been reported for estimating the CO_2 uptake of ready-mix concrete and precast concrete products cured with CO_2. This can be achieved by measuring the amount of CO_2 injected into the curing system during the production of concrete. The amount of CO_2 lost during curing needs to be measured in this method. The amount of sequestered CO_2 in concrete can be calculated by subtracting the total CO_2 lost from the total amount of CO_2 injected into the curing system. However, measuring the amount of CO_2 lost can be challenging as leakage can occur at many locations. Therefore, the assumption that the amount of CO_2 that is sequestered in the concrete is equal to the total amount injected minus the total amount lost can be significantly overstated and ideally sequestered amounts should be verified/validated by measurement in the hardened concrete product after curing. Direct measurement of uptake can also be done with CO_2 concentration measuring probes placed in the carbonation chamber. The uptake rate is evaluated by the concentration drop and the total amount of CO_2 uptake by integration of this rate. Such methods have already been proposed for other applications such as monitoring the atmospheric carbonation of recycled concrete aggregates [12, 114, 115]. A direct measurement of the uptake has the advantage of being non-destructive and allowing monitoring over time.

10 Using CO_2 uptake values in life-cycle analysis (LCA)

Two key issues in LCA studies of CO_2 utilization are additionality and temporality [116]. Since CO_2 is naturally absorbed and emitted between different natural reservoirs, a CO_2 utilization process should only be credited (i.e. to reduce CO_2 emissions) when the permanently captured CO_2 (in thermodynamically stable carbonates) is additional to the natural carbon cycle [117]. This condition applies to CO_2 utilization in cementitious materials since here CO_2 becomes chemically bound and is thermodynamically stable at ambient conditions. This additionality condition is met irrespective of whether the source of the CO_2 absorbed originates from fossil or geogenic sources, which would have otherwise increased the atmospheric CO_2 concentration; or from the air (through direct air capture or from biogenic carbon sources), which lowers the CO_2 already existing in the atmosphere [118]. While details of regulations are out of the scope of the article, EU regulations permit considering carbonation as a permanent means of carbon storage. As an example, regulation 2018/2066 [119] on the EU Emissions Trading System (ETS) permits the subtraction of CO_2 from reported (fossil) emissions when it is used to produce precipitated calcium carbonate, where the CO_2 is chemically bound. Similarly, EU Regulation 2024/3012 [120] on the voluntary certification of carbon removals, which covers atmospheric or biogenic CO_2 sources, recognizes "permanently chemically bound carbon in products" in its "permanent carbon removal" definition.

Crediting CO_2 absorbed through natural air carbonation of a cementitious material requires special consideration. This includes the significant variation in CO_2 uptake depending on its end use (e.g. indoor building decking, outdoor paving) and due to the uncertainty imparted by the temporality of natural carbonation that can span many years or even centuries (non-technical reasons significantly influence the in-use lifetime of concrete especially in buildings). Guidelines for natural recarbonation accounting are

given in EN 16757 [121]. Due to the urgency of climate change mitigation and the nature of the global warming potential of CO_2 gas which decays over time, it is more beneficial to reduce CO_2 emissions in the present than in the future [122]. Dynamic LCA, which provides a cumulative snapshot of the climate change impact over the product life cycle, is useful for studying natural carbonation especially when the time horizon for carbonation is long (as it is in natural recarbonation), but is more complex than static LCA [123, 124], and is not necessary to perform an insightful LCA study, especially for products of enforced carbonation.

CO_2 chemically bound by the cementitious material should always be included in the system boundary. The system boundary can be expanded to include the CO_2 source, or it can be modelled via a substitution allocation approach that substitutes flows of equivalent functionality, e.g., a product made from waste CO_2 mineralization substituting one made from virgin resources [125, 126]. Substitution-based allocation can hence credit the use of wastes as avoided impact from their alternate uses, e.g., landfilling. The definition of the system boundary depends on the goal and scope of each study. RILEM TC 309-MCP focuses on several LCA aspects including on carbonated recycled concrete aggregates [127].

The functional unit selected, typically a unit (e.g. 1 kg, 1 m^3) of binder, aggregates, or concrete, should reflect the function of the cementitious material produced from the CO_2 utilization process [128]. For example, Ravikumar et al. [129] used a functional unit that includes volume and 28 days compressive strength in assessing ready-mix concrete and CO_2 injected ready-mix concrete. However, considerations of mass, volume, or strength ignore durability, or, at best, indirectly account for it. Bulk resistivity could possibly be used as an indirect but rapidly measurable indicator of durability [130–132]. However, the functional unit should also be simple and in general there is no perfect choice.

Primary data should ideally be used for the specific unit processes within the main scope of the LCA study, including upstream processes such as the capture, separation, transportation, and enforcement/injection of CO_2 [26]. Indirect sources of impact such as the required infrastructure, the maintenance and monitoring of the CO_2 utilization processes, and potential CO_2 leakage during transportation, can be considered but may not be available or significantly affect the LCA study conclusions [129]. Quantities of CO_2 absorbed in the cementitious materials output by CO_2 utilization processes can be measured experimentally or modelled, as discussed earlier in this Section.

Although consideration of multiple impact categories provides a more comprehensive LCA result, it is usually justified in CO_2 utilization applications to focus on climate change, and report results at the midpoint level (global warming potential). Large uncertainty is imparted to the LCA results through the choice of LCA study parameters, therefore, carefully considered and clearly documented modelling choices regarding how allocation and CO_2 uptake is modelled, and what the basis of comparison is in a comparative LCA study, is essential for reliable quantification of the climate change mitigation potential of mineral carbonation.

11 Practical considerations and comparisons of test methods

To assess the CO_2 uptake of a process, whether natural or enforced carbonation, representative samples should be analyzed before and after the process step, or during the process. Determining the CO_2 uptake is relatively simpler for powder SCMs, but as the sample heterogeneity increases as we scale to concrete, the complexity increases profoundly. For all powder test methods, two major challenges are associated with sampling and sieving. When it is desired to measure the CO_2 uptake in a solid sample, the carbonation extent may vary as a function of depth. In such a case, the $CaCO_3$ measured at the surface and the bulk may be very different. Thus, testing of multiple powders from one specimen may be required. Even at one point, multiple test repeats are likely needed for confidence in measurements. As one goes from paste to mortar to concrete, the material heterogeneity increases, while the amount of mineralized $CaCO_3$ reduces (dilution). Interference from the presence of $CaCO_3$ in the aggregates must be overcome, as the measurement of interest is the mineralized $CaCO_3$ in the matrix but not the $CaCO_3$ that is present a priori in the aggregates. After powdering, sieving is needed. Sieving may be done in two ways, one in which the aggregates are removed, and the other

in which the entire material is ground down. In the first, incomplete removal of aggregates will cause the samples to have variable paste fractions. In the second, due to dilution, the amounts of mineralized $CaCO_3$ measured are low, and differentiation between the mineralized $CaCO_3$ and any $CaCO_3$ present in aggregates is needed. Either way, the major material sampling challenge is obtaining a representative powder in mortar/concrete without interference from the aggregates. This challenge becomes much more complex if the aggregates are limestone-based. When testing SCMs, cements, or carbonatable binders, aggregates are not a concern, however, there is interference due to the carbonates present in some binders. Thus, for accurate measurements, in addition to before/after measurements, the CO_2 content of all raw materials must be determined. When mix designs are unknown and raw materials are unavailable, determination of uptake becomes incredibly challenging, as appropriate corrections cannot be made.

In test methods where $CaCO_3$ amounts are determined, the CO_2 uptake is back-calculated. Generally, when tests such as XRD, TGA, LOI (from step-wise heating in a furnace), and combustion are compared, the amount/uptake results match well; however, careful consideration must be given to the limitations discussed previously. As an example, when using XRD, there may be an underestimation of the amount of CO_2 for materials containing amorphous $CaCO_3$. As seen in Fig. 7, the quantification of CO_2 content of a carbonated C_2S system corresponds well to the results of other independent methods such as TGA and combustion (denoted in the figure as elemental analyzer, EA). In contrast, the quantification of CO_2 content by XRD is underestimated after carbonation of a BOF slag as is apparent by comparison to results from other methods. This underestimation indicates the presence of amorphous calcium carbonates. Both examples show that XRD is instrumental in identifying different polymorphs of $CaCO_3$; FTIR and Raman can also aid with this differentiation. The BOF slag example also shows that combining XRD with TGA or other chemical techniques, enables to reveal the presence of amorphous calcium carbonate if care is taken to accurately determine the amorphous or unknown phase content. There is also the question of how the uptake should be expressed, whether normalization is by cement portion (kg CO_2/kg cement), overall concrete mass (kg CO_2/kg concrete), or by concrete volume (kg CO_2/m^3 concrete).

Tran et al. [96] applied a modified Van Slyke's method to estimate the mineralized CO_2 content of construction materials utilizing two specimen sizes (i.e., 50 mg and 200 mg). To validate the method

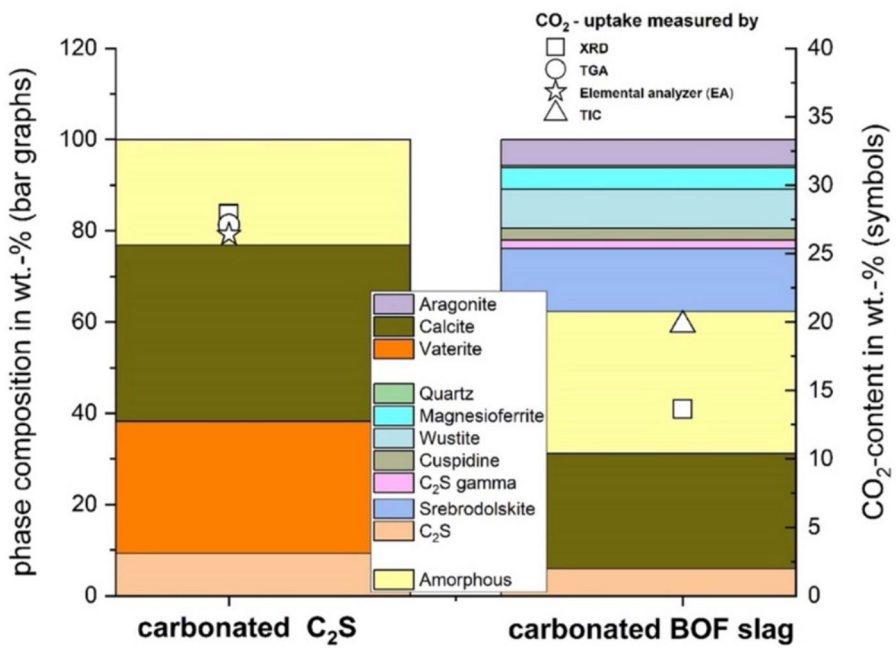

Fig.7 Phase composition and CO_2 uptake in a carbonated C_2S and BOF samples (replotted using data from [97]) showing the presence of different polymorphs of $CaCO_3$, comparison of various methods, as well as the potential underestimation of CO_2 uptake with XRD

in a robust manner, digestion-titration results were compared to TGA results. Overall, the findings demonstrated that digestion-titration results were on par with TGA results for single-phase specimens, but slightly outperformed TGA for specimens composed of multiple phases.

Apart from sampling and sieving issues, for RCA samples, drying and crushing is also required; in such cases, the time for such preparation should be minimized. In all cases, if the carbonate content is not measured immediately, the sample should be stored in a dry place, away from all moisture and CO_2. TGA or combustion analyses are generally the 'reference' methods for quantification of carbonates or CO_2 content in cementitious materials. Obtaining accurate results and ensuring the representativeness of the sample requires repeat measurements to be taken since the sample size is small. For most samples, tests are done on the powders, with certain exceptions. Measurement on larger samples is challenging, but LOI up to 950 °C, can be used to quantify CO_2 content for large samples. Considering heat transfer and other parameters, the heating rate and holding time must be tailored to the specimen size. The error of this quantification method is typically 0.5% when done in well controlled conditions, determined for recycled concrete aggregate [99].

The Fastcarb project provided recommendations and compared methods for measuring captured CO_2 at industrial scales [98–101]. It was concluded that while TGA has its uses, LOI and calcimetry methods offer more reliable and practical options for measuring CO_2 in carbonation processes. TGA is suitable when changing material sources but is complex. LOI is ideal for characterizing average batches of materials before and after carbonation. It can be used for long-duration testing (12 h) on average recycled concrete aggregate batches. Calcimetry is effective for quality control between LOI measurements for production control to correct issues such as drift in carbonator settings [98, 99]. Studies have also shown limited differences between calcimeter, thermogravimetry, and gravimetric analysis when tests have been carefully performed [133]. In general, careful sample preparation and following appropriate procedures/guidelines is critical for obtaining quantitative data in cementitious material systems [134]. As this field grows and more advances are made, careful testing, quantification, and understanding of limitations of test methods [135] will remain critical.

Table 4 shows a comparison of the various test methods discussed in the text. Mass change and measurements of CO_2 injected are not listed; we note that these are likely the methods which are most applicable for industrial process control.

Table 4 Comparison of various carbonate/CO_2 uptake test methods. Quant is quantitative, dest is destructive. The * indicates generally but not always. Cost, in USD, is an estimated cost of the equipment for a 'base' model. Given the vast variability in the parameters, the numbers listed to a certain extent are subjective

Method	Measurement	Quant?	Dest?	Speed	Cost	Range/Error
TGA	CO_2 mass loss, can be converted to carbonates	Yes	Yes	2 h	$50,000	< 1% $CaCO_3$
LOI	Mass loss, can be converted to CO_2 (or carbonates)	Yes	Yes	2 h	$5,000	0.5% Error
Combustion/CS	Carbon mass loss, can be converted to CO_2	Yes	Yes	5 min	$50,000	< 1% CO_2 Repeatability < 2% single operator
NMR	Information about polymorphs	No	No	2 h	$500,000	–
FTIR	Peaks give info about polymorphs and amorphous $CaCO_3$	No*	No*	5 min	$50,000	–
Raman		No*	Yes/No	Variable	$300,000	–
XRD	Peaks give info about polymorphs and amounts	Yes	Yes*	30 min	$100,000	Precision 1 – 5%
Chemical methods	Volume, pressure, or mass changes converted to CO_2	Yes	Yes	Variable	$5,000 or below	1 mg $CaCO_3$ Variable

12 Summary

All concrete uptakes CO_2, as do other cement-based materials. Also, intentionally carbonated construction products use and permanently store CO_2. Reliably quantifying the climate change mitigation potential of mineral carbonation products requires accurate measurement of their CO_2 uptake. TGA, LOI, combustion analysis, NMR, FTIR, Raman, XRD, chemical methods, mass change, measurement of CO_2 injected, can all be used to measure CO_2 (or carbonate) content. Of these methods, NMR, FTIR, and Raman are generally not quantitative. TGA and combustion analysis are the most commonly used for quantification purposes. At an industrial scale, combustion, mass change, and measurement of CO_2 injected are likely the only ones that are feasible. When using powder, representative sampling is critical; contamination/dilution from aggregates in concrete products or aggregates complicates measurements. To accurately determine CO_2 uptake, measurements before and after CO_2 exposure are needed, or, alternatively, measurements on raw materials. Through the use of complementary methods, as an example, the use of XRD to determine the $CaCO_3$ polymorphs, accurate quantification and an understanding of mechanisms can be obtained. Further round-robin testing, comparing the various methods is an urgent need to advance measurements, including in the lab, industrial scales, and in the field.

Acknowledgements The authors thank the following for their contributions: Alisa Machner (TU Munich), Fabian Niewoehner (TU Munich), Vilma Ducman (ZAG—Slovenian National Building and Civil Engineering Institute), Isabel Martins (Laboratório Nacional de Engenharia Civil), Fernanda Belizario Silva (ETH Zurich), and Yury Villagran-Zaccardi (VITO NV). RS acknowledges support by the Horizon Europe–Widening project ASCCENT under grant agreement 101159895.

Author contributions Conceptualization: E. Garboczi, T. Matschei, R. Snellings. Coordination: T. Matschei, R. Snellings, P. Suraneni. Formal Analysis, Investigation, Visualization, and Writing—original draft: Sections leads as follows, Sect. 1, 11: T. Matschei, P. Suraneni, Sect. 2: B. Huet, Sect. 3: B. Scruggs, Sect. 4, 5, 6: N. Garg, Sect. 7: D. Jansen, Sect. 8: S. Braymand, Sect. 9, 10: R.J. Myers. Writing—review and editing: All authors, lead P. Suraneni.

Funding Horizon Europe Widening Participation and Strengthening the European Research Area, 101159895, Ruben Snellings

Declarations

Conflict of interest Ellina Bernard, Ippei Maruyama, and Prannoy Suraneni are Associate Editors of Materials and Structures. The authors declare no competing interests in this publication.

Open Access This article is licensed under a Creative Commons Attribution 4.0 International License, which permits use, sharing, adaptation, distribution and reproduction in any medium or format, as long as you give appropriate credit to the original author(s) and the source, provide a link to the Creative Commons licence, and indicate if changes were made. The images or other third party material in this article are included in the article's Creative Commons licence, unless indicated otherwise in a credit line to the material. If material is not included in the article's Creative Commons licence and your intended use is not permitted by statutory regulation or exceeds the permitted use, you will need to obtain permission directly from the copyright holder. To view a copy of this licence, visit http://creativecommons.org/licenses/by/4.0/.

References

1. Radha AV, Forbes TZ, Killian CE, Gilbert PUPA, Navrotsky A (2010) Transformation and crystallization energetics of synthetic and biogenic amorphous calcium carbonate. Proc Natl Acad Sci U S A 107(38):16438–16443
2. Siva T, Muralidharan S, Sathiyanarayanan S, Manikandan E, Jayachandran M (2017) Enhanced polymer induced precipitation of polymorphous in calcium carbonate: calcite aragonite vaterite phases. J Inorg Organomet Polym Mater 27:770–778
3. Photong C, Pragot W (2022) Effect of adding monohydrocalcite on the microstructural change in cement hydration. ACS Omega 7(41):36318–36329
4. Tian L, Tahmasebi A, Yu J (2014) An experimental study on thermal decomposition behavior of magnesite. J Therm Anal Calorim 118(3):1577–1584
5. Gallagher PK, Warne SSJ (1981) Thermomagnetometry and thermal decomposition of siderite. Thermochim Acta 43(3):253–267
6. Hartman M, Svoboda K, Pohořelý M, Šyc M (2013) Thermal decomposition of sodium hydrogen carbonate and textural features of its calcines. Ind Eng Chem Res 52(31):10619–10626
7. Hartman M, Svoboda K, Čech B, Pohořelý M, Šyc M (2019) Decomposition of potassium hydrogen carbonate: thermochemistry, kinetics, and textural changes in solids. Ind Eng Chem Res 58(8):2868–2881
8. Villagran Zaccardi, Y., Eguez Alava, H., De Buysser, K. and De Belie, N., 2017. On the quantitative thermogravimetric analysis of calcite content in hydrated cementitious systems. In: *14th International Conference on Durability of Building Materials and Components (XIV DBMC),* pp. 1–6.

9. Kim T, Olek J (2012) Effects of sample preparation and interpretation of thermogravimetric curves on calcium hydroxide in hydrated pastes and mortars. Transp Res Rec 2290(1):10–18
10. Takahashi H et al (2023) Error factors in quantifying inorganic carbonate CO_2 in concrete materials. J Adv Concr Technol 21(10):789–802
11. Igami R, Igarashi G, Aili A, Daisuke M, Kurihara R, Maruyama I (2025) Clinker mineral formation and thermal decomposition of calcium carbonates in carbonated tobermorites: mechanism of CO_2 release in low-temperature ranges. Cem Concr Res 197:107969
12. Hou Y, Turcry P, Mahieux PY, Cazacliu B, Lux J, Aït-Mokhtar A (2025) A comparative study of CO_2 uptake quantification methods: a case study on recycled concrete aggregates under natural carbonation. J Build Eng 101:111845
13. Maruyama I, Noritake K, Hosoi Y, Takahashi H (2024) Development of a large-scale thermogravimetry and gas analyzer for determining carbon in concrete. J Adv Concr Technol 22(6):383–390
14. Walloch, C., Powers, L., Broton, D. and Thompson, J., 2022. Conceptual test protocols for measuring carbon sequestration of manufactured dry-cast concrete products. In Masonry 2022: Advancing Masonry Technology (pp. 59–86). 100 Barr Harbor Drive, PO Box C700, West Conshohocken, PA 19428–2959: ASTM International.
15. *ASTM E1019–24* – Standard test methods for determination of carbon, sulfur, nitrogen, and oxygen in steel, iron, nickel, and cobalt alloys by various combustion and inert gas fusion techniques, ASTM International, West Conshohocken, PA, 2024.
16. *ASTM C114–24* – Standard test methods for chemical analysis of hydraulic cement, ASTM International, West Conshohocken, PA, 2024.
17. Bennet EL, Harley JH, Fowler RM (1950) Conductometric method for determination of carbon in steel. Anal Chem 22(3):445–448
18. B. Scruggs, WK80282 update: Standard test method for determination of CO_2 in cements and concretes, ASTM C01 Meeting, Denver, CO, 2023.
19. *ASTM WK80282* – New standard test method for determination of CO_2 in cements and concretes, ASTM International, West Conshohocken, PA, 2024.
20. Zhang Z, Scherer GW (2021) Physical and chemical effects of isopropanol exchange in cement-based materials. Cem Concr Res 145:106461
21. Kahn, L., 1988. Determination of total organic carbon in sediment. *United States Environmental Protection Agency,* Region II, Environmental Services Division, Monitoring Management Branch, Edison, NJ.
22. Skibsted J, Hall C (2008) Characterization of cement minerals, cements and their reaction products at the atomic and nano scale. Cem Concr Res 38(2):205–225
23. Walkley B, Provis JL (2019) Solid-state nuclear magnetic resonance spectroscopy of cements. Mater Today Adv 1:100007
24. Neto FM, Snellings R, Skibsted J (2024) Aqueous carbonation of aged blended Portland cement pastes: impact of the Al/Si ratio on the structure of the alumina-silica gel. Cem Concr Res 177:107428
25. Skibsted, J., 2016. High-resolution solid-state nuclear magnetic resonance spectroscopy of Portland cement-based systems. Chapter 6 In: A Practical Guide to Microstructural Analysis of Cementitious Materials, Eds. K. Scrivener, R. Snellings, B. L. Lothenbach, CRC Press, pp. 213 – 286.
26. Zajac M, Skocek J, Skibsted J, Haha MB (2021) CO_2 mineralization of demolished concrete wastes into a supplementary cementitious material–a new CCU approach for the cement industry. RILEM Tech Lett 6:53–60
27. Zajac M, Song J, Ullrich P, Skocek J, Haha MB, Skibsted J (2024) High early pozzolanic reactivity of alumina-silica gel: a study of the hydration of composite cements with carbonated recycled concrete paste. Cem Concr Res 175:107345
28. Sevelsted TF, Herfort D, Skibsted J (2013) ^{13}C chemical shift anisotropies for carbonate ions in cement minerals and the use of ^{13}C, ^{27}Al and ^{29}Si MAS NMR in studies of Portland cement including limestone additions. Cem Concr Res 52:100–111
29. Papenguth HW, Kirkpatrick RJ, Montez B, Sandberg PA (1989) ^{13}C MAS NMR spectroscopy of inorganic and biogenic carbonates. Am Mineral 74(9–10):1152–1158
30. Michel FM, MacDonald J, Feng J, Phillips BL, Ehm L, Tarabrella C, Parise JB, Reeder RJ (2008) Structural characteristics of synthetic amorphous calcium carbonate. Chem Mater 20(14):4720–4728
31. Bernard E, Lothenbach B, Rentsch D, German A, Winnefeld F (2022) Effect of carbonates on the formation of magnesium silicate hydrates. Mater Struct 55(7):183
32. Moore JK, Surface JA, Brenner A, Skemer P, Conradi MS, Hayes SE (2015) Quantitative identification of metastable magnesium carbonate minerals by solid-state ^{13}C NMR spectroscopy. Environ Sci Technol 49(1):657–664
33. Chang CF, Chen JW (2006) The experimental investigation of concrete carbonation depth. Cem Concr Res 36(9):1760–1767
34. Martínez-Ramírez S, Fernández-Carrasco L (2012) Carbonation of ternary cement systems. Constr Build Mater 27(1):313–318
35. Qin L, Gao X, Chen T (2019) Influence of mineral admixtures on carbonation curing of cement paste. Constr Build Mater 212:653–662
36. Zajac M, Skibsted J, Skocek J, Durdzinski P, Bullerjahn F, Haha MB (2020) Phase assemblage and microstructure of cement paste subjected to enforced, wet carbonation. Cem Concr Res 130:105990
37. Zajac M, Skibsted J, Durdzinski P, Bullerjahn F, Skocek J, Haha MB (2020) Kinetics of enforced carbonation of cement paste. Cem Concr Res 131:106013
38. dos Santos VHJM et al (2021) Application of Fourier Transform infrared spectroscopy (FTIR) coupled with multivariate regression for calcium carbonate ($CaCO_3$) quantification in cement. Constr Build Mater 313:125413
39. Regev L, Poduska KM, Addadi L, Weiner S, Boaretto E (2010) Distinguishing between calcites formed by different mechanisms using infrared spectrometry: archaeological applications. J Archaeol Sci 37(12):3022–3029

40. Chakrabarty D, Mahapatra S (1999) Aragonite crystals with unconventional morphologies. J Mater Chem 9(11):2953–2957
41. Veerasingam S, Venkatachalapathy R (2014) Estimation of carbonate concentration and characterization of marine sediments by Fourier transform infrared spectroscopy. Infrared Phys Technol 66:136–140
42. Wang X et al (2019) High-temperature Raman and FTIR study of aragonite-group carbonates. Phys Chem Miner 46:51–62
43. Signorelli S, Peroni C, Camaiti M, Fratini F (1996) The presence of vaterite in bonding mortars of marble inlays from Florence Cathedral. Mineral Mag 60(401):663–665
44. Andersen FA, Brecevic L, Beuter G, Dell'Amico DB, Calderazzo F, Bjerrum NJ, Underhill AE (1991) Infrared spectra of amorphous and crystalline calcium carbonate. Acta Chem Scand 45(10):1018–1024
45. Lázár A et al (2023) Insights into the amorphous calcium carbonate (ACC)→ ikaite→ calcite transformations. CrystEngComm 25(5):738–750
46. Coleyshaw EE, Crump G, Griffith WP (2003) Vibrational spectra of the hydrated carbonate minerals ikaite, monohydrocalcite, lansfordite and nesquehonite. Spectrochim Acta A Mol Biomol Spectrosc 59(10):2231–2239
47. Shen P et al (2022) Phase assemblance evolution during wet carbonation of recycled concrete fines. Cem Concr Res 154:106733
48. Wang X, Xu X, Ye Y, Wang C, Liu D, Shi X, Wang S, Zhu X (2019) In-situ high-temperature XRD and FTIR for calcite, dolomite and magnesite: anharmonic contribution to the thermodynamic properties. J Earth Sci 30:964–976
49. Dubrawski JV, Channon AL, Warne SSJ (1989) Examination of the siderite-magnesite mineral series by Fourier transform infrared spectroscopy. Am Mineral 74(1–2):187–190
50. Mi T et al (2021) Quantitative evaluation of cement paste carbonation using Raman spectroscopy. npj Mater Degrad 5(1):35
51. Li Y et al (2022) Assessment of compositional changes of carbonated cement pastes subjected to high temperatures using in-situ Raman mapping and XPS. J Build Eng 45:103454
52. Addadi L, Raz S, Weiner S (2003) Taking advantage of disorder: amorphous calcium carbonate and its roles in biomineralization. Adv Mater 15(12):959–970
53. Goto S, Maruyama I (2023) Carbonation of cement hydrates under different relative humidity environments evaluated by micro-Raman spectroscopy. J Soc Mater Sci Jpn 72(5):361–368
54. Zou Z et al (2019) A hydrated crystalline calcium carbonate phase: calcium carbonate hemihydrate. Sci 363(6425):396–400
55. Bischoff WD, Sharma SK, MacKenzie FT (1985) Carbonate ion disorder in synthetic and biogenic magnesian calcites: a Raman spectral study. Am Mineral 70(5–6):581–589
56. DeCarlo TM (2018) Characterizing coral skeleton mineralogy with Raman spectroscopy. Nat Commun 9(1):5325
57. Black L (2009) Raman spectroscopy of cementitious materials. Spectrosc Properties Inorganic Organometallic Compdounds 40:72–127
58. Stefaniuk D, Hajduczek M, Weaver JC, Ulm FJ, Masic A (2023) Cementing CO_2 into C-S-H: a step toward concrete carbon neutrality. PNAS Nexus 2(3):pgad052
59. Srivastava S, Garg N (2023) Tracking spatiotemporal evolution of cementitious carbonation via Raman imaging. J Raman Spectrosc 54(4):414–425
60. Mario M et al (2021) Portable quantitative confocal Raman spectroscopy: non-destructive approach of the carbonation chemistry and kinetics. Cem Concr Res 139:106280
61. Zhang K, Yio MHN, Wong HS, Buenfeld NR (2022) Optimising confocal Raman microscopy for spectral mapping of cement-based materials. Mater Struct 55(4):131
62. Polavaram KC, Garg N (2021) Enabling phase quantification of anhydrous cements via Raman imaging. Cem Concr Res 150:106592
63. Dufresne WJ, Rufledt CJ, Marshall CP (2018) Raman spectroscopy of the eight natural carbonate minerals of calcite structure. J Raman Spectrosc 49(12):1999–2007
64. Boulard E, Guyot F, Fiquet G (2012) The influence on Fe content on Raman spectra and unit cell parameters of magnesite–siderite solid solutions. Phys Chem Miner 39(3):239–246
65. Frost RL (2011) Raman spectroscopic study of the magnesium carbonate mineral hydromagnesite ($Mg_5[(CO_3)_4(OH)_2]\cdot 4H_2O$). J Raman Spectrosc 42(8):1690–1694
66. Rathnakumar S, Garg N (2024) Multi-modal imaging of the cementitious carbonation front: evidence for pore refinement. J CO2 Util 90:102993
67. Singer M, van Geldern R, Barth JA, Jansen D (2024) Advancements in enforced C_2S wet carbonation: leveraging δ13C isotope tracking for reaction insights. J CO2 Util 88:102924
68. Snellings R, Bazzoni A, Scrivener K (2014) The existence of amorphous phase in Portland cements: physical factors affecting Rietveld quantitative phase analysis. Cem Concr Res 59:139–146
69. Cheng L et al (2024) Plugging effect of fine pore water in OPC and LC^3 paste during accelerated carbonation monitored via single-sided nuclear magnetic resonance spectroscopy. Cem Concr Res 186:107688
70. Cheng L et al (2025) Mechanisms of change in accelerated carbonation progress in cement paste under different relative humidity conditions. Cem Concr Res 195:107898
71. Ouyang X, Wang L, Xu S, Ma Y, Ye G (2020) Surface characterization of carbonated recycled concrete fines and its effect on the rheology, hydration and strength development of cement paste. Cem Concr Compos 114:103809
72. Lu B, Shi C, Zhang J, Wang J (2018) Effects of carbonated hardened cement paste powder on hydration and microstructure of Portland cement. Constr Build Mater 186:699–708
73. Saeki N, Kurihara R, Maruyama I (2024) Applicability of XRD/Rietveld analysis with an external standard

method for the quantification of mineral components in carbonated hardened cement paste. J Adv Concr Technol 22(10):602–619
74. Jansen D, Stabler C, Goetz-Neunhoeffer F, Dittrich S, Neubauer J (2011) Does ordinary Portland cement contain amorphous phase? a quantitative study using an external standard method. Powder Diffr 26(1):31–38
75. Gholizadeh-Vayghan A, Snellings R (2022) Beneficiation of recycled concrete fines through accelerated carbonation. Mater Struct 55(7):171
76. Salman M et al (2014) Effect of accelerated carbonation on AOD stainless steel slag for its valorisation as a CO_2-sequestering construction material. Chem Eng J 246:39–52
77. Santos RM, Van Bouwel J, Vandevelde E, Mertens G, Elsen J, Van Gerven T (2013) Accelerated mineral carbonation of stainless steel slags for CO_2 storage and waste valorization: effect of process parameters on geochemical properties. Int J Greenh Gas Control 17:32–45
78. Bodor M, Santos RM, Kriskova L, Elsen J, Vlad M, Van Gerven T (2013) Susceptibility of mineral phases of steel slags towards carbonation: mineralogical, morphological and chemical assessment. Eur J Mineral 25(4):533–549
79. Snellings R, Machiels L, Mertens G, Elsen J (2010) Rietveld refinement strategy for quantitative phase analysis of partially amorphous zeolitized tuffaceous rocks. Geol Belg 13:183–196
80. De Silva P, Bucea L, Sirivivatnanon V (2009) Chemical, microstructural and strength development of calcium and magnesium carbonate binders. Cem Concr Res 39(5):460–465
81. Le Saoût G, Kocaba V, Scrivener K (2011) Application of the Rietveld method to the analysis of anhydrous cement. Cem Concr Res 41(2):133–148
82. Baciocchi R, Costa G, Di Gianfilippo M, Polettini A, Pomi R, Stramazzo A (2015) Thin-film versus slurry-phase carbonation of steel slag: CO_2 uptake and effects on mineralogy. J Hazard Mater 283:302–313
83. Sherrod LA, Dunn G, Peterson GA, Kolberg RL (2002) Inorganic carbon analysis by modified pressure-calcimeter method. Soil Sci Soc Am J 66(1):299–305
84. Gualtieri AF, Viani A, Montanari C (2006) Quantitative phase analysis of hydraulic limes using the Rietveld method. Cem Concr Res 36(2):401–406
85. *NF P94–098* – Détermination de la teneur en carbonate, méthode du calcimètre, AFNOR Edition, France, 1996, 12pp [In French].
86. Head KH (1998) Manual of soil laboratory testing, Volume 2: permeability, shear strength and compressibility tests. Pentech Press Limited, London, pp 278–290
87. Muller G (1971) The "Karbonat-Bombe", a simple device for the determination of the carbonate content in sediments, soils and other materials. Neues Jahrb Mineral 10:466–469 (**[In German]**)
88. Braymand, S., Roux, S. 2024. Investigation of the CO_2 sequestration by accelerated carbonation as a function of the composition, origin, production process, and age of recycled concrete aggregates. In: *12th ACI/RILEM International Conference on Cementitious Materials and Alternative Binders for Sustainable Concrete*, pp.1062.
89. Unluer C, Al-Tabbaa A (2014) Enhancing the carbonation of MgO cement porous blocks through improved curing conditions. Cem Concr Res 59:55–65
90. Unluer C, Al-Tabbaa A (2015) The role of brucite, ground granulated blastfurnace slag, and magnesium silicates in the carbonation and performance of MgO cements. Constr Build Mater 94:629–643
91. Pu L, Unluer C (2016) Investigation of carbonation depth and its influence on the performance and microstructure of MgO cement and PC mixes. Constr Build Mater 120:349–363
92. Ferrara G, Belli A, Keulen A, Tulliani JM, Palmero P (2023) Testing procedures for CO_2 uptake assessment of accelerated carbonation products: experimental application on basic oxygen furnace steel slag samples. Constr Build Mater 406:133384
93. Bonfante F, Ferrara G, Humbert P, Garufi D, Tulliani JMC, Palmero P (2024) CO2 sequestration through aqueous carbonation of electric arc furnace slag. J Adv Concr Technol 22(4):207–218
94. Bonfante F, Humbert P, Tulliani JM, Palmero P, Ferrara G (2024) CO2 uptake of cement by-pass dust via direct aqueous carbonation: an experimental design for time and temperature optimisation. Mater Struct 57(8):181
95. Van Slyke DD (1918) The determination of carbon dioxide in carbonates. J Biol Chem 36(2):351–354
96. Tran, T.Q., Cook, R., Ipindoala, O., Fanijo, E.O., Newman, A., Stutzman, P.E. and Brand, A.S., Measuring mineralized carbon in carbonate minerals and cementitious materials by an acid digestion-titration method. *Preprint available at SSRN 4860805*.
97. Librandi P, Nielsen P, Costa G, Snellings R, Quaghebeur M, Baciocchi R (2019) Mechanical and environmental properties of carbonated steel slag compacts as a function of mineralogy and CO_2 uptake. J CO2 Util 33:201–214
98. Braymand S., Mercado Menoza H., Roux S., 2023. Étude paramétrique de l'évolution des propriétés des granulats recyclés lors de la carbonatation et élaboration d'une base de données collaborative des résultats. *Fastcarb Research Report*, 119pp [In French].
99. Fastcarb French National Project, 2024. Stockage de CO_2 dans les Granulats de Béton Recyclé – Recommandations du PN FastCarb; *Project Rep*ort, In Press [In French].
100. Torrenti JM et al (2022) The FastCarb project: taking advantage of the accelerated carbonation of recycled concrete aggregates. Case Stud Constr Mater 17:e01349
101. Izoret L, Pernin T, Potier JM, Torrenti JM (2023) Impact of industrial application of fast carbonation of recycled concrete aggregates. Appl Sci (Basel) 13(2):849
102. Steinour, H.H., 1956. The ultimate products of the carbonation of portland cement. *Research Department of Portland Cement Association.*
103. De Weerdt K, Plusquellec G, Revert AB, Geiker MR, Lothenbach B (2019) Effect of carbonation on the pore solution of mortar. Cem Concr Res 118:38–56
104. Zajac M, Skibsted J, Lothenbach B, Bullerjahn F, Skocek J, Haha MB (2022) Effect of sulfate on CO_2 binding efficiency of recycled alkaline materials. Cem Concr Res 157:106804

105. Srivastava S, Snellings R, Cool P (2021) Clinker-free carbonate-bonded (CFCB) products prepared by accelerated carbonation of steel furnace slags: a parametric overview of the process development. Constr Build Mater 303:124556
106. Baciocchi R, Costa G, Di Bartolomeo E, Polettini A, Pomi R (2010) Carbonation of stainless steel slag as a process for CO_2 storage and slag valorization. Waste Biomass Valor 1:467–477
107. Ghouleh Z, Guthrie RI, Shao Y (2015) High-strength KOBM steel slag binder activated by carbonation. Constr Build Mater 99:175–183
108. Mahoutian M, Shao Y (2016) Production of cement-free construction blocks from industry wastes. J Clean Prod 137:1339–1346
109. Nielsen P, Quaghebeur M (2023) Determination of the CO_2 uptake of construction products manufactured by mineral carbonation. Minerals 13(8):1079
110. Huijgen WJ, Witkamp GJ, Comans RN (2005) Mineral CO_2 sequestration by steel slag carbonation. Environ Sci Technol 39(24):9676–9682
111. Moon EJ, Choi YC (2018) Development of carbon-capture binder using stainless steel argon oxygen decarburization slag activated by carbonation. J Clean Prod 180:642–654
112. Mo L, Zhang F, Deng M (2016) Mechanical performance and microstructure of the calcium carbonate binders produced by carbonating steel slag paste under CO_2 curing. Cement Concr Res 88:217–226
113. Li L, Wu M (2022) An overview of utilizing CO_2 for accelerated carbonation treatment in the concrete industry. J CO2 Util 60:102000
114. Boumaaza M, Huet B, Turcry P, Aït-Mokhtar A (2020) The CO2-binding capacity of synthetic anhydrous and hydrates: validation of a test method based on the instantaneous reaction rate. Cement Concr Res 135:106113
115. Engelsen, C.J., Mehus, J., Pade, C. and Sæther, D.H., 2005. Carbon dioxide uptake in demolished and crushed concrete. Project report, 395.
116. Arcusa S, Sprenkle-Hyppolite S (2022) Snapshot of the carbon dioxide removal certification and standards ecosystem (2021–2022). Clim Policy 22(9–10):1319–1332
117. Brandão M et al (2013) Key issues and options in accounting for carbon sequestration and temporary storage in life cycle assessment and carbon footprinting. Inter J Life Cycle Assessment 18:230–240
118. Wang X, Song C (2020) Carbon capture from flue gas and the atmosphere: a perspective. Front Energy Res 8:560849
119. Document 32018R2066: Commission Implementing Regulation (EU) 2018/2066 of 19 December 2018 on the monitoring and reporting of greenhouse gas emissions pursuant to Directive 2003/87/EC of the European Parliament and of the Council and amending Commission Regulation (EU) No 601/2012.
120. Document 32024R3012: Regulation (EU) 2024/3012 of the European Parliament and of the Council of 27 November 2024 establishing a Union certification framework for permanent carbon removals, carbon farming and carbon storage in products.
121. EN 16757, 2022. Sustainability of construction works—Environmental product declarations—Product category rules for concrete and concrete elements. CO2 Uptake by Carbonation—Guidance on Calculation.
122. Sedjo, R.A., 2013. Comparative life cycle assessments: carbon neutrality and wood biomass energy. *Resources for the Future DP*, pp.13–11.
123. Hoxha, E. and Passer, A., 2021, November. Should biogenic carbon be analysed separately in the calculation of the GWP indicator? In: *Journal of Physics: Conference Series* (Vol. 2042, No. 1, p. 012168). IOP Publishing.
124. Van Roijen E, Sethares K, Kendall A, Miller SA (2024) The climate benefits from cement carbonation are being overestimated. Nat Commun 15(1):4848
125. Marinković S, Josa I, Braymand S, Tošić N (2023) Sustainability assessment of recycled aggregate concrete structures: a critical view on the current state-of-knowledge and practice. Struct Concr 24(2):1956–1979
126. Heijungs R et al (2021) System expansion and substitution in LCA: a lost opportunity of ISO 14044 amendment 2. Front Sustain 2:692055
127. Belizario-Silva F, et al., 2025. Life cycle assessment of carbonated recycled concrete aggregates: a critical review and recommendations (in preparation). *Mater Structures*.
128. Hafez H, Kurda R, Al-Ayish N, Garcia-Segura T, Cheung WM, Nagaratnam B (2021) A whole life cycle performance-based ECOnomic and ECOlogical assessment framework (ECO2) for concrete sustainability. J Clean Prod 292:126060
129. Ravikumar D, Zhang D, Keoleian G, Miller S, Sick V, Li V (2021) Carbon dioxide utilization in concrete curing or mixing might not produce a net climate benefit. Nat Commun 12(1):855
130. Sengul O (2014) Use of electrical resistivity as an indicator for durability. Constr Build Mater 73:434–441
131. Azarsa P, Gupta R (2017) Electrical resistivity of concrete for durability evaluation: A review. Adv Mater Sci Eng 2017(1):8453095
132. Wang Y, Ramanathan S, Chopperla KST, Ideker JH, Suraneni P (2022) Estimation of non-traditional supplementary cementitious materials potential to prevent alkali-silica reaction using pozzolanic reactivity and bulk resistivity. Cem Concr Compos 133:104723
133. Kavcic N, Tominc S, Zibret L, Zibret G, Kolar M, Ducman V (2025) Comparing methods for determining the CO_2 content in CO_2-sequestering materials and natural rock. Ceram Int. https://doi.org/10.1016/j.ceramint.2025.07.109. (**in press**)
134. Scrivener K, Snellings R, Lothenbach B (2016) A practical guide to microstructural analysis of cementitious materials, vol 540. CRC Press, Boca Raton, FL, USA
135. Qiu Q (2020) A state-of-the-art review on the carbonation process in cementitious materials: fundamentals and characterization techniques. Constr Build Mater 247:118503

Publisher's Note Springer Nature remains neutral with regard to jurisdictional claims in published maps and institutional affiliations.